AMERICAN UNIVERSITY OF BEIRUT

PROTEOMIC ANALYSIS OF BRADYKININ SIGNALING IN PODOCYTES

by
RICHARD SUHEIL SAOUD

A thesis
submitted in partial fulfillment of the requirements
for the degree of Master of Science
to the Department of Biochemistry and Molecular Genetics
of the Faculty of Medicine
at the American University of Beirut

Beirut, Lebanon
September 2017

AMERICAN UNIVERSITY OF BEIRUT

PROTEOMIC ANALYSIS OF BRADYKININ SIGNALING IN PODOCYTES

by

RICHARD SUHEIL SAOUD

Approved by:

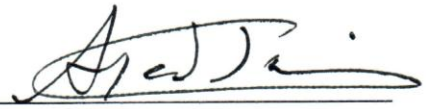

Dr. Ayad Jaffa, Professor — Advisor
Biochemistry and Molecular Genetics
American University of Beirut

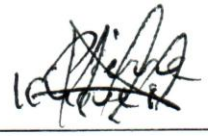

Dr. Pierre Khoueiry. Assistant Professor — Co-Advisor
Biochemistry and Molecular Genetics
American University of Beirut

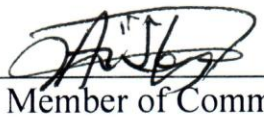

Dr. Aida Habib, Professor — Member of Committee
Biochemistry and Molecular Genetics
American University of Beirut

Dr. Assaad Eid, Associate Professor — Member of Committee
Anatomy, Cell Biology, and Physiology
American University of Beirut

Date of thesis defense: September 22, 2017

AMERICAN UNIVERSITY OF BEIRUT

THESIS, DISSERTATION, PROJECT RELEASE FORM

Student Name:

SAOUD	RICHARD	SUHEIL
Last	First	Middle

● Master's Thesis ○ Master's Project ○ Doctoral Dissertation

☐ I authorize the American University of Beirut to: (a) reproduce hard or electronic copies of my thesis, dissertation, or project; (b) include such copies in the archives and digital repositories of the University; and (c) make freely available such copies to third parties for research or educational purposes.

■ I authorize the American University of Beirut, to: (a) reproduce hard or electronic copies of it; (b) include such copies in the archives and digital repositories of the University; and (c) make freely available such copies to third parties for research or educational purposes after:

One ---- year from the date of submission of my thesis, dissertation, or project.
Two ---- years from the date of submission of my thesis, dissertation, or project.
Three -X- years from the date of submission of my thesis, dissertation, or project.

Richard 24/11/2017

Signature Date

This form is signed when submitting the thesis, dissertation, or project to the University Libraries

ACKNOWLEDGMENTS

First, I would like to thank my thesis advisor Dr. Ayad Jaffa, for giving me the opportunity to join his lab to fulfill my thesis requirements for my Masters of Science. I want to thank him for being an encouraging advisor that helped me to become the independent scientist I am today, and for being exceedingly patient at times where experimental progress was slow.

I would like to express my gratitude to my friends at the lab: Mostafa al Hariri, Fatima Ghamlouche, Ola Dagher, and Abeer Ayoub, for teaching me the laboratory techniques that I have performed in the frame of my thesis work. I admit that my stay at the lab was very smooth because of their friendly demeanor and helpful spirit.

I would also like to thank Dr. Aida Habib for always providing me with advice, whether the subject matter was academic or not, and for aiding me in troubleshooting my experiments.

I would like to thank Dr. Nadine Darwiche for her invaluable support during my first year of study. Her support helped me to pass a very difficult time in my life, and for that, I am grateful.

I would like to thank the committee members Dr. Pierre Khoueiry and Dr. Assaad Eid for agreeing to supervise my thesis progress and for evaluating my thesis defense and providing me with their insightful corrections and comments to my thesis.

I would like to express my gratitude to my friend Timo Kroes for his consistent support and encouragement.

Finally, I would like to thank my family: My father Suheil, my mother Mangala, and my sister Grace. No words could express my gratitude for their never-ending support and love. I love you all so very much.

AN ABSTRACT OF THE THESIS OF

Richard Suheil Saoud for Master of Science
Major: Biochemistry and Molecular Genetics

Title: Proteomic Analysis of Bradykinin Signaling in Podocytes

Background and Aim: Diabetic end-stage nephropathy is the main cause of long-term death for diabetic patients. Podocyte damage is one of the hallmarks of diabetic nephropathy, where the loss of the podocyte filtration barrier leads to proteinuria and progressive renal damage. Research on Kallikrein Kinin System (KKS) has integrated its way into diabetic nephropathy research, where the fluctuations of the signaling molecules in this system have been shown to alter certain aspects of the disease. Bradykinin (BK) is a vasoactive peptide that was shown to play an important role in the progression of renal damage. In this study, we aim to evaluate the changes in protein expression profiles of rat podocytes upon the treatment with BK by Mass Spectrometry in conjunction with pathway enrichment analysis. This analysis will help in discovering core effectors whose upstream and downstream protein profile can elucidate the signaling mechanisms underlying BK's modulation of the podocyte biology.

Methods: Cultured immortalized rat podocytes were treated with BK at 10^{-7} M for 3 and 6 hours. Protein profile was evaluated by LC-MS/MS analysis, and pathway enrichment analysis was performed on the output data. The discovery of the upregulation of cyclo-oxygenase 2 (COX-2) prompted us to measure COX-2 protein and activity levels by western blot and enzyme immunoassay respectively, as well as identifying players in the BK/COX-2 signaling pathway by western blot.

Results: BK treatment showed the up- and down-regulation of multiple proteins, where COX-2 was upregulated. Pathway enrichment analysis was performed on the proteomics data to broaden our understanding of the cellular processes occurring upon BK stimulation. We confirmed the upregulation of the COX-2 protein and activity levels using western blot and enzyme immuno-assay, and showed that the BK stimulation of COX-2 is downstream the MAPK pathway. We identified the downregulation of Nephrin upon to BK stimulation. Finally, using the enzyme immunoassay technique, we observed that the upregulation of PGE_2 production in response to BK treatment is by a COX-2 and MAPK-dependant mechanisms.

Conclusion: Proteomic analysis of podocytes treated by BK revealed the up- and down-regulation of 61 proteins, among them the upregulation of COX-2. Pathway enrichment analysis suggested an inhibition of the cell death pathway and the involvement of elements of the cytoskeletal activity. Western blot analysis and the EIA technique confirmed the upregulation of the COX-2 protein expression and activity levels. Furthermore, they confirmed the upregulation of phospho ERK as part of the same pathway and the downregulation of Nephrin. And finally, that BK's stimulation of PGE_2 production was inhibited in the presence of an ERK inhibitor and a COX inhibitor. This reveals BK as an important modulator in the arachidonic acid metabolism pathway and a potential player in the progression of diabetic nephropathy.

CONTENTS

ILLUSTRATIONS

Figure Page

TABLES

Table Page

CHAPTER I

INTRODUCTION

A. Diabetes Mellitus:

1. Statistics:

Diabetes has become one of the most studied diseases of our time due to its impact on human life and the medical economy. The World Health Organization reports in its 2016 "Global report on diabetes" an astonishing number of 422 million adults living with diabetes in 2014, presenting as a 3.9-fold increase from 108 million back in 1980. Diabetes totaled 3.7 million deaths in 2012, 1.5 million of which were directly attributed to diabetes and the other 2.2 million caused by hyperglycemia-related diseases such as cardiovascular complications and others. Of these deaths, 43% of the people were under the age of 70 [1]. Noteworthy trends in the pattern of diabetes prevalence among populations include an increased mortality attributed to high blood glucose from all-cause deaths among members of the lower middle-income group, as well as the geographical difference in the prevalence of diabetes, peaking in the eastern Mediterranean region populations. As for the impact on the medical and healthcare economy, according to the American Diabetes Association, the 2012 cost of diagnosed diabetes in the United States has been estimated at $245 billion split between $176 billion in medical costs and $69 billion in the correlated reduction in productivity[2].

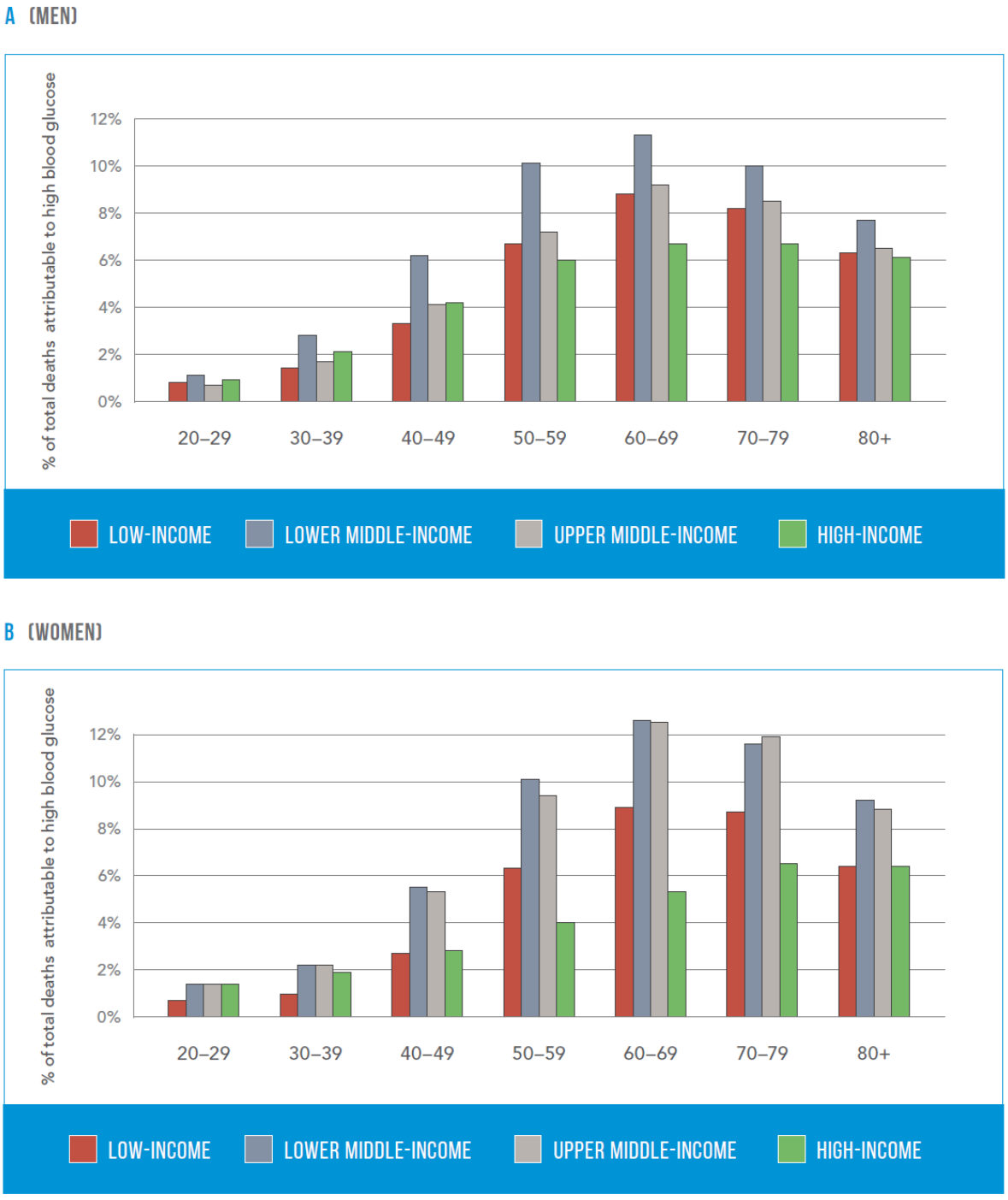

Figure 1: Mortality percentage of total deaths attributed to hyperglycemia by age and country income group for men and women, retrieved from WHO's 2016 Global Report on Diabetes in 2012 [1].

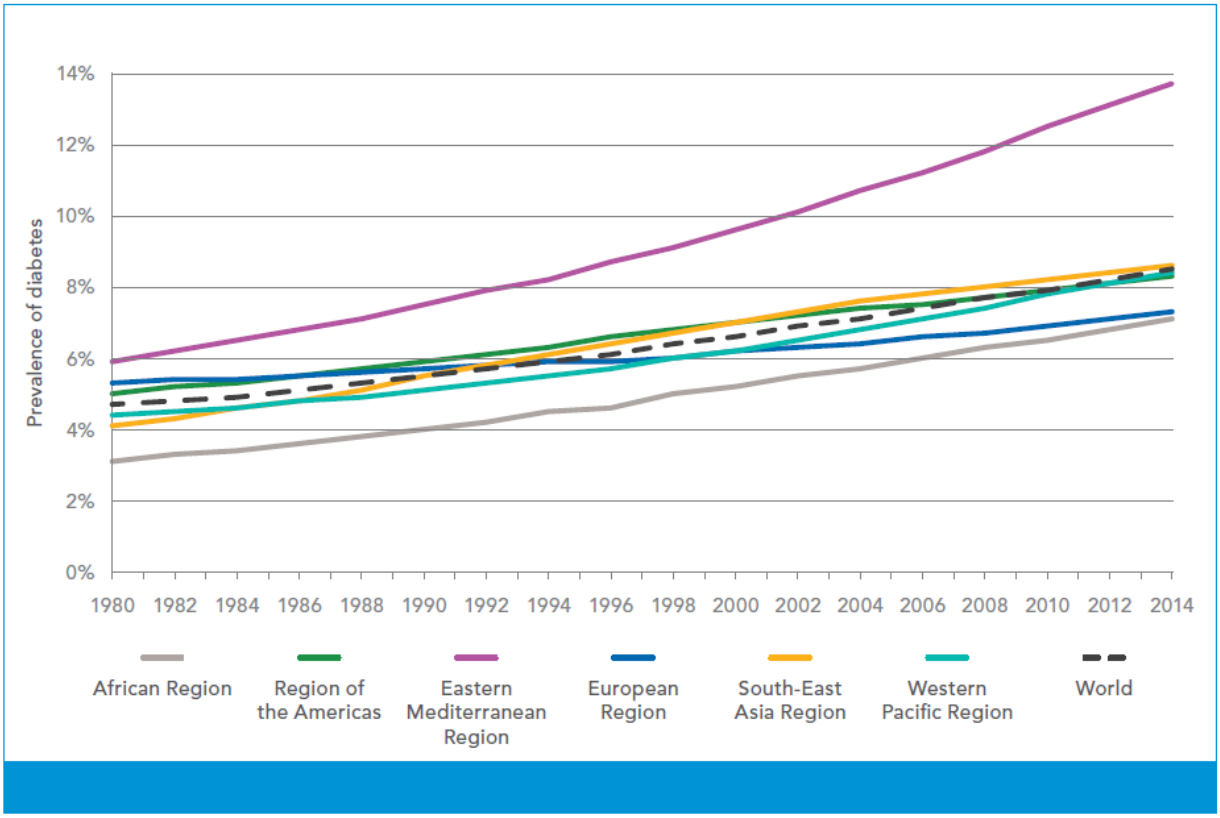

Figure 2: Trends in the prevalence of diabetes through 1980-2014 across WHO regions [1].

2. Types of Diabetes Mellitus:

Historically, Diabetes Mellitus has been classified into 2 subtypes: Type-1 Diabetes Mellitus characterized by the inability of the body to secrete insulin due to autoimmune attacks on the body's β-cells in the pancreas and early onset age, and Type-2 Diabetes Mellitus characterized by the body's lack of sensitivity to insulin [3]. However, more recent studies have suggested new classifications of diabetes based on the onset age, mode of inheritance, and genetic variabilities. Latent autoimmune diabetes of adults is characterized by the presentation with type-2 diabetes mellitus features, but with the

presence of pancreatic auto-immune antibodies. Maternally inherited diabetes and deafness is associated with the mitochondrial m.3243A>G mutation [4]. Gestational diabetes mellitus is characterized by its onset during the second or third trimester and its dissipation following childbirth, and by the fact that it's considered a risk factor for the development of type-2 diabetes mellitus [5]. Finally, monogenic variations of diabetes mellitus (such as maturity-onset diabetes of the young, or MODY) is caused by a mutation in the gene HNF1A coding for the transcription factor hepatic nuclear factor 1-α which regulates glucose metabolism as well as insulin secretion [3]. This section sheds light on the difficulty of diabetes as a disease, as it hints at the complexity of the underlying signaling mechanisms that fall under the common hyperglycemic phenotype.

3. Organ Pathology:

a. General Organ Pathology:

While the complex cascade of protein signaling and interactions linking the chronic hyperglycemic state to the long term symptoms associated with diabetes mellitus have not been fully elucidated, one of the proposed mechanisms involve the formation of advanced glycation end products (AGEs) [6,7]. This theory suggests that the hyperglycemic state leads to the formation of glycation products when glucose forms covalent bonds with plasma proteins [7]. This irreversible modification of plasma proteins (collagen, fibrinogen, albumin, and globulins) causes dysfunctions in the protein activity, and lead to pathological effects in different organs when the AGEs accumulate and interact with their receptors (RAGEs: receptors for advanced glycation end products) [6]. Many receptors have been

identified as RAGEs, such as lactoferrin, oligosaccharyl transferase-48 (OST-48), galectin-3, CD36, and scavenger receptors types I and II [7].

But as mentioned before, even though we don't fully understand the mechanisms underlying the pathological propagation of diabetes, the chronic hyperglycemia can cause a wide array of pathological responses for different organs in the body. We will briefly go over some of the organs affected by diabetes before we move on to diabetic nephropathy.

Vascular Complications: Diabetes mellitus is considered one of the major risk factors for the development of multiple vascular diseases, including myocardial infarction, stroke, and other peripheral vascular diseases [8], with type-1 diabetic patients having a higher risk of developing coronary events earlier due to the early onset of type-1 diabetes mellitus [9]. According to a collaborative meta-analysis of 102 prospective studies, diabetics have a two-fold increased risk for a wide array of vascular diseases aside from the conventional risk factors that occur with diabetes like obesity and hypertension [10,11]. The possible existence of a difference in risk of developing coronary heart disease between men and women is still under debate, where according to one meta-analysis on 37 prospective studies, women have a 50% higher relative risk for diabetes-associated fatal coronary heart disease [12], while another meta-analysis on 8 prospective studies indicated that the excess relative risk of developing coronary heart disease for women vs men becomes absent after adjusting for classic coronary heart disease risk factors [13].

Most of the different organ pathologies linked to the chronic hyperglycemic level fall under 2 categories: microvascular and macrovascular complications. [14,15]. Microvascular complications include diabetic neuropathy, retinopathy, and nephropathy

while macrovascular complications include coronary artery disease, peripheral vascular disease, and cerebrovascular diseases [14]. I will briefly mention the microvascular pathologies as I make my way to diabetic nephropathy.

Retinopathy: Diabetic retinopathy falls under the classification of microvascular complications associated with diabetes mellitus [16]. It is the leading cause of blindness among working-aged adults around the world [17,18], with its risk factors being identified as hyperglycemia, hypertension, and dyslipidemia [19]. The suggested microvascular complications has been said to lead to non-perfusion, hypoxia, and the ensuing breakdown of the blood-retinal barrier [16].

Neuropathy: The most common form of diabetic neuropathy (affecting at least 50% of diabetics [20]) is peripheral neuropathy where diabetic patients can present different symptoms that can range from sensory loss in the toes to severe pain neuropathy [21]. Another type of diabetic neuropathy is autonomic neuropathy, characterized by resting tachycardia, orthostatic hypotension, exercise intolerance, and an increased mortality risk in the presence of cardiac autonomic neuropathy [22].

b. Diabetic Nephropathy:

Diabetic nephropathy (DN) is the leading cause of end-stage renal disease [23], and it has long been thought that the high mortality due to cardiovascular disease in diabetics with nephropathy suggested a strong association between microvascular and macrovascular pathologies in diabetes [24]. Classic signs of the progression of nephropathy include the severity of albuminuria (≥ 30mg/day) [25], and the estimated glomerular filtration rate (eGFR) to a lesser extent [26]. Other suggested biomarkers for progression of renal damage have included the levels of urinary Smad3 protein [27], while the vasoconstrictor peptide Endothelin-1 has been independently associated with decreasing GFR in patients with diabetic nephropathy [28]. Also, it is suggested that the previously-mentioned accumulation of AGEs and their receptors RAGEs correlates with the severity of the diabetic nephropathy [21,29]. Anatomically, it has been established that podocyte loss is a hallmark of diabetic nephropathy [30], while mesangial matrix expansion [31] and a reduction in glomerular endothelial fenestration have also been correlated with its progression [32]. We will focus on Podocyte damage in the scope of diabetic nephropathy, as my project revolves around the study of podocytes on the molecular level in response to different conditions of treatment.

Podocytes are epithelial cells that line the Bowman's capsule in the glomerulus, that are in contact with the glomerular capillaries. They form the third barrier of filtration in the glomerulus, preceded by the fenestrated glomerular endothelial cells and the glomerular basement membrane. Podocytes possess a large number of foot processes forming slits, which fluid filters in after passing through the first two barriers of filtration. These slits don't allow large molecules such as proteins, to pass through, while small molecules like

water and salts are excreted. The podocyte slit diaphragm serves as a signaling hub for the podocytes where many molecules interact and are produced such as Laminin β2, Collagen α3α4α5, and the proangiogenic factors VEGF-A and Angiopoetin-1. Many structural proteins are at the core of the slit diaphragm, which are responsible for regulating the reactive elements of the glomerular filtration system, and in turn are the cause of serious renal damage when dysfunctions occur within their signaling systems.

Many proteins have been studied and linked to podocyte physiology and pathology, whether in the frame of diabetic nephropathy or other pathologies with podocyte involvement. I will discuss past and ongoing research on some of these proteins to better elucidate the complicated signaling mechanisms underlying podocyte physiology.

Connective Tissue Growth Factor (CTGF) has been demonstrated to play a role in vascular and renal damage in a multifactorial hypertension model [33]. Another study has suggested that podocyte injury in spontaneously hypertensive is mediated, at least in part, by CTGF [34]. Another study supported this hypothesis by showing that in puromycin aminonucleoside nephrosis (PAN) rats, CTGF and its mRNA were both highly upregulated in podocytes, and this upregulation correlated with development of proteinuria in acute PAN conditions, and with high expression of fibronectin (FN), collagens I, III, & IV, and glomerulosclerosis in chronic PAN conditions [35]. Moreover, this study showed the increased expression of mRNA for Transforming Growth Factor β (TGF-β), while another study re-suggested the relation between TGF-β and CTGF [36]. One paper showed that CTGF and Integrin-linked Kinase (ILK) were both upregulated in high-glucose condition in a time-dependant and dose-dependent manner, and the study also suggested that ILK acts as a downstream effector of CTGF [37]. One study suggested a possible relation between

upregulation of CTGF in diabetic nephropathy conditions with the reduction in podocyte markers (WT1, Nephrin, and Synaptopodin) [38]. A clinical study suggested the downregulation of CTGF following podocyte loss in diabetic nephropathy conditions [39].

Nephrin is one of the structural proteins that are active at the podocyte slit diaphragm. The NPHS1 gene encodes podocyte-expressed immunoglobulin superfamily protein Nephrin, whose mutations can cause congenital nephrotic syndrome in humans [40]. While Nephrin is one of the structural proteins at the slit diaphragm, it also plays a role in the signaling occurring at the diaphragm, where Nephrin, along with its associated proteins, control the development, cytoskeletal architecture, shape, and viability of the podocytes, and by extension, the function of the filtration barrier [41,42].

One final protein of interest that has been associated with podocyte injury is Cyclooxygenase 2 (COX-2). This protein is suggested to be linked to podocyte injury, where an increased exposure of podocytes to albumin caused an upregulation in COX-2 mRNA and protein level [43]. This protein and its ties to diabetic nephropathy and podocyte injury will be discussed in detail in the inflammation section of this introduction.

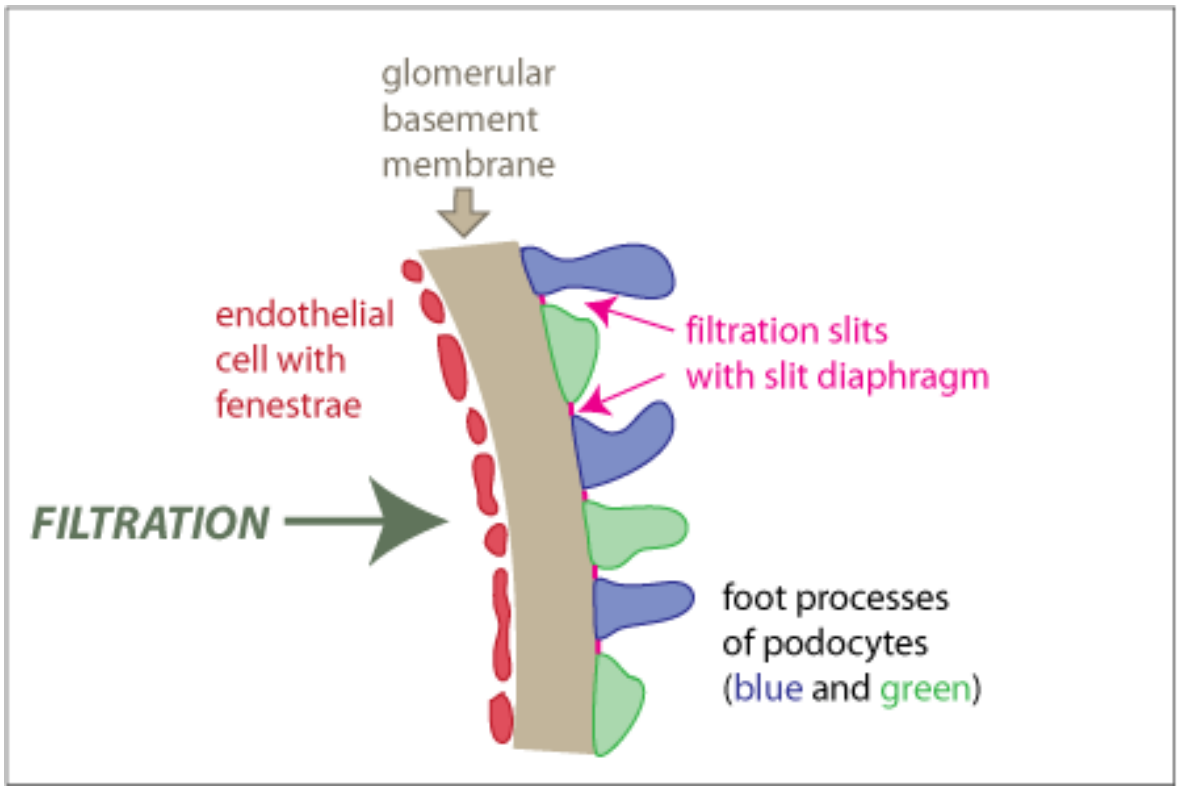

Figure 3: Illustration depicting the elements forming the glomerular filtration system, retrieved from the University of Washington's online course.

B. Kallikrein-Kinin system:

The Kallikrein-Kinin system is a family of signaling molecules that play an important role in physiological and pathological events such as hypertension regulation, the coagulation response, inflammation, cardiovascular disease, and diabetes. I will start with an introduction of the family members before moving on to their roles in pathology, and specifically, diabetic nephropathy.

1. Kallikreins:

The Kallikrein family of serine proteases is generally divided into 2 species: the Plasma Kallikrein (PK) coded by the gene Klkb, and the Tissue Kallikrein family encoded by the gene KLK1, part of the tissue kallikrein-related peptidases which encompass 15 proteins that have at least 30% sequence identity [44]. We will discuss both.

c. Plasma Kallikrein (PK):

As mentioned before, plasma kallikrein is a serine protease that is primarily synthesized in the liver, and to a lesser extent in the pancreas, kidneys, adrenal glands, and the placenta, as the abundant-circulating glycoprotein zymogen plasma prekallikrein (PPK) [45,46]. PPK is activated by Factor XIIa primarily, or by prolylcarboxypeptidase (PRCP) on the surface of endothelial cells (as demonstrated in the human umbilical endothelial cells (HUVEC)) [47-49], resulting in the PPK being cleaved at Arg371 leading to the disulfide-linked heavy and light chains conformation, exposing the protein-binding domain and reveals its catalytic activity [46]. The activated PK is now able to cleave its primary substrates, namely high molecular weight kininogen (HK), which 75-90% of PK is found circulating with in the plasma, into Bradykinin (BK), and Factor XII, converting it to the activated Factor XIIa [45].

PK intersects many signaling pathways, either through its products or by itself. These pathways include the kallikrein-kinin system (KKS) (to be discussed later in the introduction), the intrinsic coagulation pathway, the fibrinolytic pathway, the alternative complement system, the renin-angiotensin system (RAS), [45], and the adipogenesis pathway [46]. I'll briefly mention PK's involvement in these systems:

The Intrinsic Coagulation Pathway:

We have mentioned before that PK and Factor XII reciprocally activate each other. Downstream of that, FXIIa activates FXI. FXIa leads to calcium-dependant activation of FIX, thereby promoting coagulation. FX serves as the converging point of the intrinsic and extrinsic coagulation pathways, where FXa, while in a complex with FVa, generates thrombin from the prothrombin zymogen, which leads to downstream activation of multiple pathways in the vascular system, as well as converting fibrinogen to fibrin [45,50].

Fibrinolysis:

As a counter-balance to the coagulation pathway, the fibrinolysis pathway leads to the dissolution of the fibrin network. PK's role in the system is the indirect activation of fibrinolysis by activating the proenzyme of urokinase-type plasminogen activator (uPA), which converts the precursor plasminogen into the active molecule plasmin, which plays the main role in dissolving the fibrin networks [51]. While it has been shown in vitro that PK converts plasminogen to plasmin directly (using a buffer system), the in vivo PK-mediated direct activation of plasmin remains to be demonstrated [45].

Alternative Complement Pathway:

In the activation of the alternative pathway C3 convertase of the human complement, PK can replace factor D, whose job is to cleave factor B, part of the active C3bBb. This is not of major importance though, as factor D is 10 times more effective at cleaving factor B than PK at a per-mole basis. The importance of PK within this system has not been thoroughly explored in vivo, yet some individuals with deficiencies

in the contact factors (PK, FXII, FXI, and HK) have been reported to have increased likelihood of getting bacterial infections [45,52].

Adipogenesis:

The same involvement of PK-mediated activation of plasminogen in the fibrinolysis pathway has been suggested to also play a role in adipocyte differentiation and adipogenesis during the mammary gland involution step of development through the cleavage of the preadipocyte stromal matrix by plasmin [46,53].

The Renin-angiotensin System:

The renin-angiotensin system (RAS) (also called renin-angiotensin-aldosterone system) is a system that controls blood pressure and fluid balances within the body, and it is closely associated with the KKS, where plasma kallikrein converts prorenin to renin, which in turn converts angiotensinogen to angiotensin I, later transformed to angiotensin II by the Angiotensin-Converting Enzyme (ACE). The ACE pathway is considered vasoconstrictive, where angiotensin II is known to have a hypertensive effect on the blood vessels by producing aldosterone, which causes sodium and water resorption in the kidneys, and ACE acts as a kininase that degrades the vasodilator Bradykinin (BK) [54]. Thus, the RAS and the KKS form a blood pressure regulation system, where an imbalance between these 2 systems can lead to pathological outcomes [55].

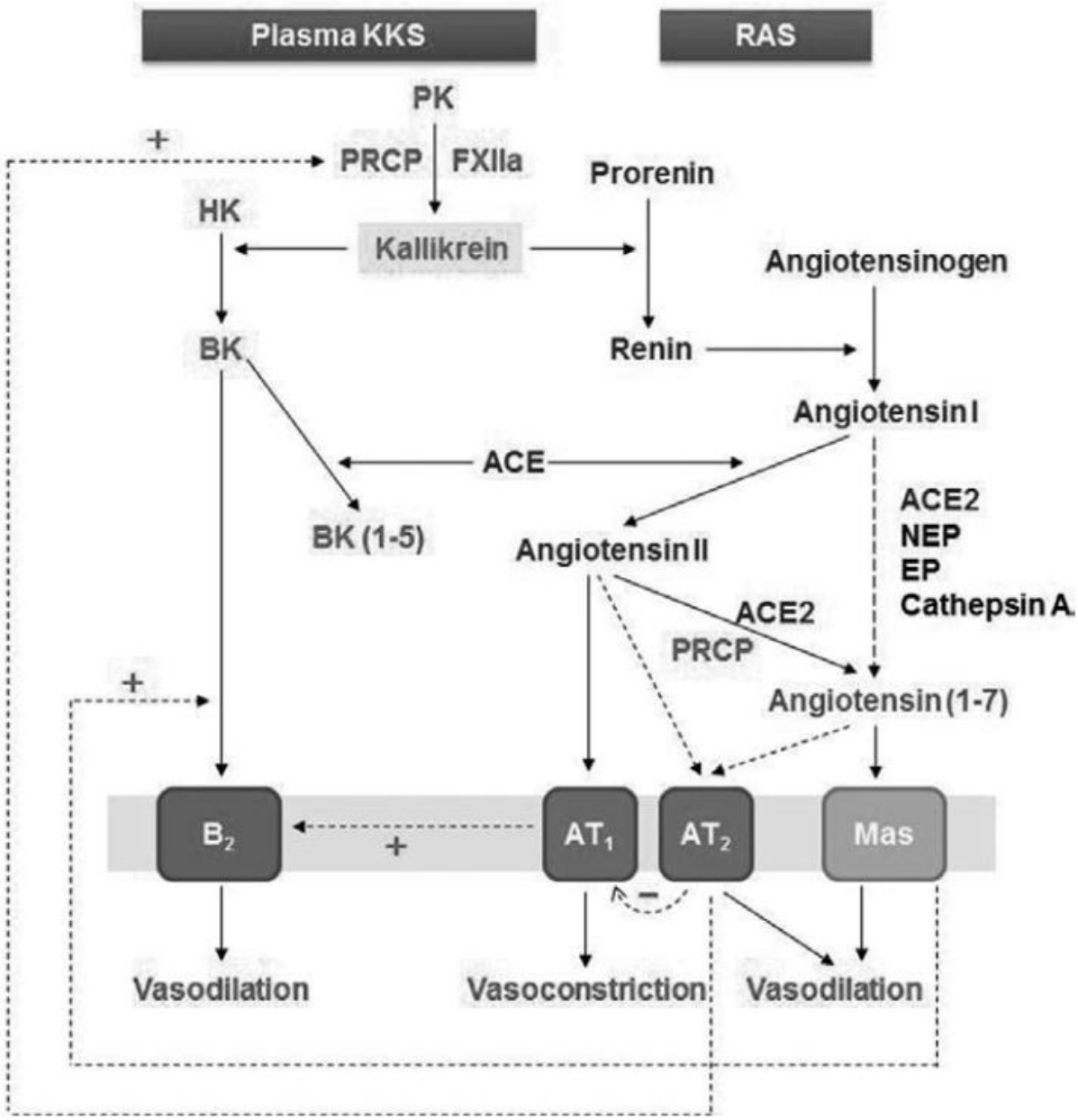

Figure 4: The multi-faceted interactions between the KKS and RAS in the frame of regulating blood pressure. Abbreviations: PK: Plasma Kallikrein; PRCRP: Prolylcarboxypeptidase; HK: High molecular weight kininogen; BK: Bradykinin; ACE: Angiotensin-converting enzyme; ACE-2: Angiotensin-converting enzyme 2; NEP: neprilysis; EP: Endopeptidases; B_2: Bradykinin B2 receptor; AT_1 & AT_2: Angiotensin receptor Type 1 & 2; Mas: Mas receptor. Retrieved from Plasma Kallikrein Inhibitors in Cardiovascular disease: An innovative Therapeutic Approach [48]

d. Tissue Kallikrein:

Human tissue kallikrein (KLK1) was the first tissue kallikrein described in the 1930s, where it was observed in the pancreas and named after this organ (pancreas is "kallikreas" in Greek), is part of the three "classical" KLKs along with KLK2 and KLK3 (which is also known as prostate cancer antigen (PSA)). These three tissue kallikreins, and primarily KLK1, have generally similar activity to PK, but instead cleave low molecular weight kininogen (LK) to produce lysyl-bradykinin (Lys-BK, also known as Kallidin) which can be further processed by arginine aminopeptidase to give BK [56]. These three tissue kallikreins have been characterized also to be from the tissue kallikrein family, composed of 15 members, along with the kallikrein-related peptidases denoted KLK4-15. However, even though these tissue kallikreins have structural similarities, KLK1 is the only tissue kallikrein with a reported significant kininogenase activity [56]. Tissue kallikreins are synthesized as zymogens that are proteolytically cleaved to generate the active conformation by the release of a hydrophobic Leucine or Isoleucine which inserts into the protease core domain [44].

2. Kinins/BK:

As mentioned before, Kinins are generated by the action of Kallikreins on Kininogens, where PK binds to HK to generate BK, and KLK1 binds to LK to generate Kallidin (Lys-BK), where Kallidin can be further cleaved by arginine aminopeptidase to generate BK, and BK and Kallidin can be cleaved by kininase to generate des-Arg9-BK. BK is a nonapeptide that is that is rapidly metabolized by several endogenous

metalloproteases, such as ACE, carboxypeptidase N (CPN), aminopeptidase P, and neutral endopeptidase (NEP) [57].

Kinins mediate their effect through the actions of the 2 G-Protein Coupled Receptors: the B1 Receptor (B1R) and the B2 Receptor (B2R) [58]. The B2R is constitutively expressed with a fast agonist desensitization action and bias to BK binding, while the B1R is an inducible receptor with a slow agonist desensitization and bias to des-Arg9-binding [57,58]. BK activation and binding to these GPCRs can mediate a plethora of downstream effects through the $G_{\alpha q/11}$ and G_i in addition to GPCR-independent BK action on different organs including vasodilation, increased vascular permeability, and the reduction of oxidation stress when it binds to B2R on endothelial cells through the effect of NO release, increased intracellular Ca^{2+} concentration (within seconds of BK binding), and prostacyclin (PgI) production [57].

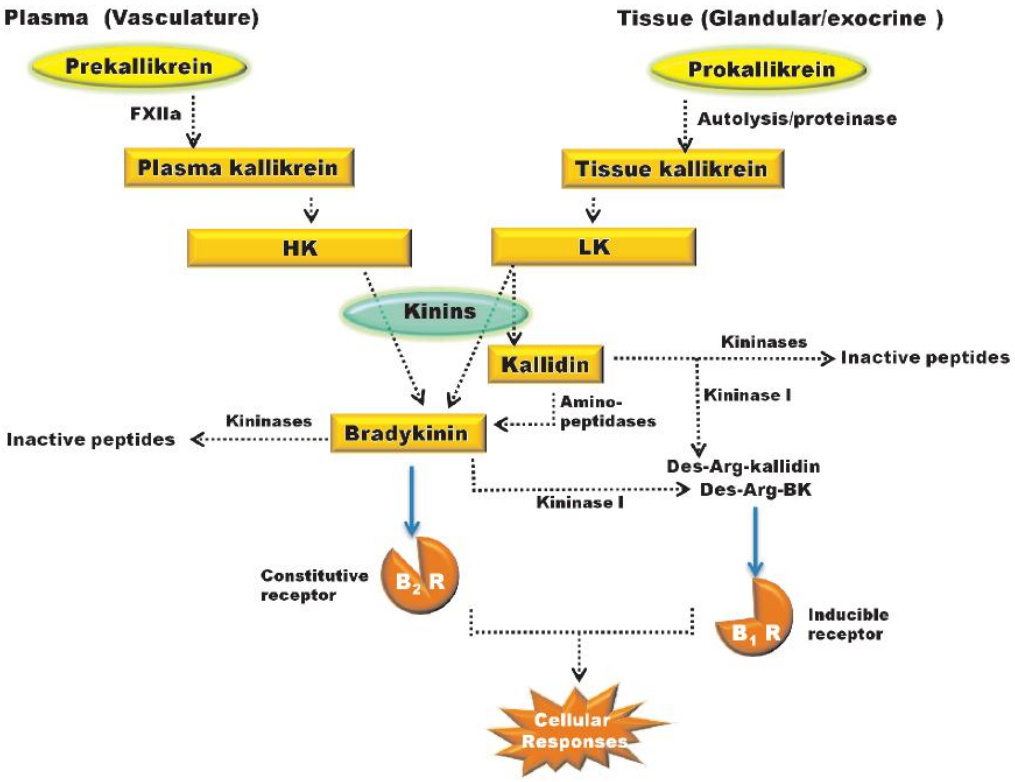

Figure 5: The KKS players: PK, KLK, and Kininogens interact to further downstream targets through the actions of the vasopeptides Bradykinin and Kallidin, and are inactivated by kininases. Abbreviations: HK: high molecular weight kininogen; LK: low molecular weight kininogen; B_1R & B_2R: Bradykinin 1&2 receptors. Retrieved from Structure of Plasma and Tissue Kallikrein [44]

3. KKS Pathology:

Elements of the KKS have been implicated in a multitude of diseases other than diabetes over the years, such as cardiovascular diseases (including thrombosis and atherosclerosis), hypertension, inflammation, cancer, central nervous system disease, and angiogenesis. For the purpose of our study, I will be reviewing the literature discussing the involvement of the KKS in diabetes.

One study has indicated that activated partial thromboplastin time (aPTT), whose prolonged duration is a well-established marker for plasma kallikrein deficiency [59], was

inversely correlated with fasting plasma glucose (FPG) and glycated hemoglobin (HbA1c) levels [46]. Another study reported the increase of PPK and factor XII's activities were increased in diabetes [60].

One study implicated the activity of PK in diabetic retinopathy, where a comprehensive proteomic analysis of several groups of people with and without proliferative retinopathy and diabetes showed increased levels of carbonic anhydrases (>8 fold increase), where the vitreous gel found in individuals with advanced stages of the disease has extracellular carbonic anhydrase as a major component. Thus this enzyme plays a pivotal role in the development of the disease, where its activity leads to increased vascular permeability in the retina and vision impairment later on. The connection between the carbonic anhydrase and the KKS is suggested to be the activation of PPK to PK through the carbonic anhydrase-mediated increase in the intraocular pH levels, resulting in increased vascular permeability via BK-mediated action. As a confirmation, the increase in vascular permeability associated with the increase in carbonic anhydrase was abrogated with the induction of FXII and PK inhibitors, B2R inhibitors, as well as the control of the intraocular pH [45]. Another study on diabetic retinopathy and diabetic macular edema showed that the abrogation of the KKS elements was an effective method to attenuate retinal vascular permeability. This study also mentions that a phase I human trial of a novel PK inhibitor for diabetic macular edema treatment is ongoing to assess the safety of this approach [61].

The role of the KKS and its elements in diabetic nephropathy is a controversial topic, with studies reporting both deleterious and protective effects brought on by BK and its receptors. For instance, a study by Jaffa et al. suggested the involvement of the KKS in

diabetic nephropathy by knocking out the B2R and measuring plasma glucose levels and albumin excretion rate. The experiment showed that diabetic mice with B2R KO had a pronounced decrease in albumin excretion rate compared to diabetic mice with wild-type B2R [62]. Another study reported the reduction in albumin excretion in a streptozocin-induced diabetic mouse model [63]. On the other hand, a study on akita mice showed that the lack of the B2R caused the mice to develop albuminuria, accompanied by an increase in glomerular mesangial sclerosis [64], and the lack of both B1R and B2R in the same akita mouse model leads to a more damaging effect including glomerulosclerosis and GBM thickening alongside the increased albuminuria [65]. These conflicting findings might be due to BK receptor expression differences in the studied tissues, or due to differences in the genetics of the different models used [48]. However, both studies showed the upregulation of the B1R expression in diabetic mice with B2R knockout [48,63,64].

Finally, BK has been known to possess a role in inflammation. In physiological situations, it is thought that BK possesses an anti-inflammatory role, where in one study set in the pleural cavity of mice, it is shown to downregulate lipopolysaccharide-induced eosinophil accumulation [66].

C. Inflammation/Cyclooxygenase-2:

The role of the inflammatory molecule cyclooxygenase-2 (COX-2) in diabetic nephropathy as well as the involvement of BK in inflammation necessitates the study of the arachidonic acid branch of metabolism. Arachidonic acid metabolism plays a major role in inflammation, with its pathways being elucidated long ago. Arachidonic acid is liberated

from the membrane phospholipids by the actions of Phospholipase A2. Arachidonic acid can also be synthesized from diacylglycerol by the actions of diacylglycerol lipase [67]. AA can then be converted into multiple families of metabolites through the actions of different enzymes.

Downstream metabolites of arachidonic acid form the eicosanoid family, comprised of the prostanoids, leukotrienes, isoprostanes, epoxyeicosatrienoic acids, lipoxins, and metabolites of 12, 15, and 5-lypoxeygenases. Arachidonic acid is released from the plasma membrane phospholipids by phospholipase A_2 (PLA_2) and is metabolized to give the unstable intermediate prostaglandin G_2 by the COX enzyme's cyclooxygenase activity, which is then converted to prostaglandin H_2 by the enzyme's peroxidase activity [68]. COX has multiple isozymes, namely COX-1 and COX-2. COX-3's identification has been a subject of debate (also sometimes called COX-1b), as some consider it a splice variant of the COX-1 gene, and it is believed to be non-functional in humans [69]. These enzymes catalyze the rate-limiting steps in the formation of prostaglandin molecules from arachidonic acid [70]. The major differences between the COX-1 and COX-2 enzymes is in expression patterns, where COX-2 is rapidly upregulated in inflammatory situations [71], while COX-1 is constitutively expressed and is thought to be the homeostatic isoform (except in the cases of some brain injuries, where it is thought to be actively involved) [72]. An interesting study showed that COX-2 transgenic streptozocin-induced diabetic mice developed progressive albuminuria with their hyperglycemia, blood pressure, and glomerular filtration rate being similar to wild-type [73].

The downstream metabolite PGH_2 serves as a precursor for the production of other metabolites including the downstream prostanoids PGE_2, PGD_2, $PGF_{2\alpha}$, PGI_2 in addition to thromboxane A_2, each produced by its own tissue specific enzymes and isomerases [69].

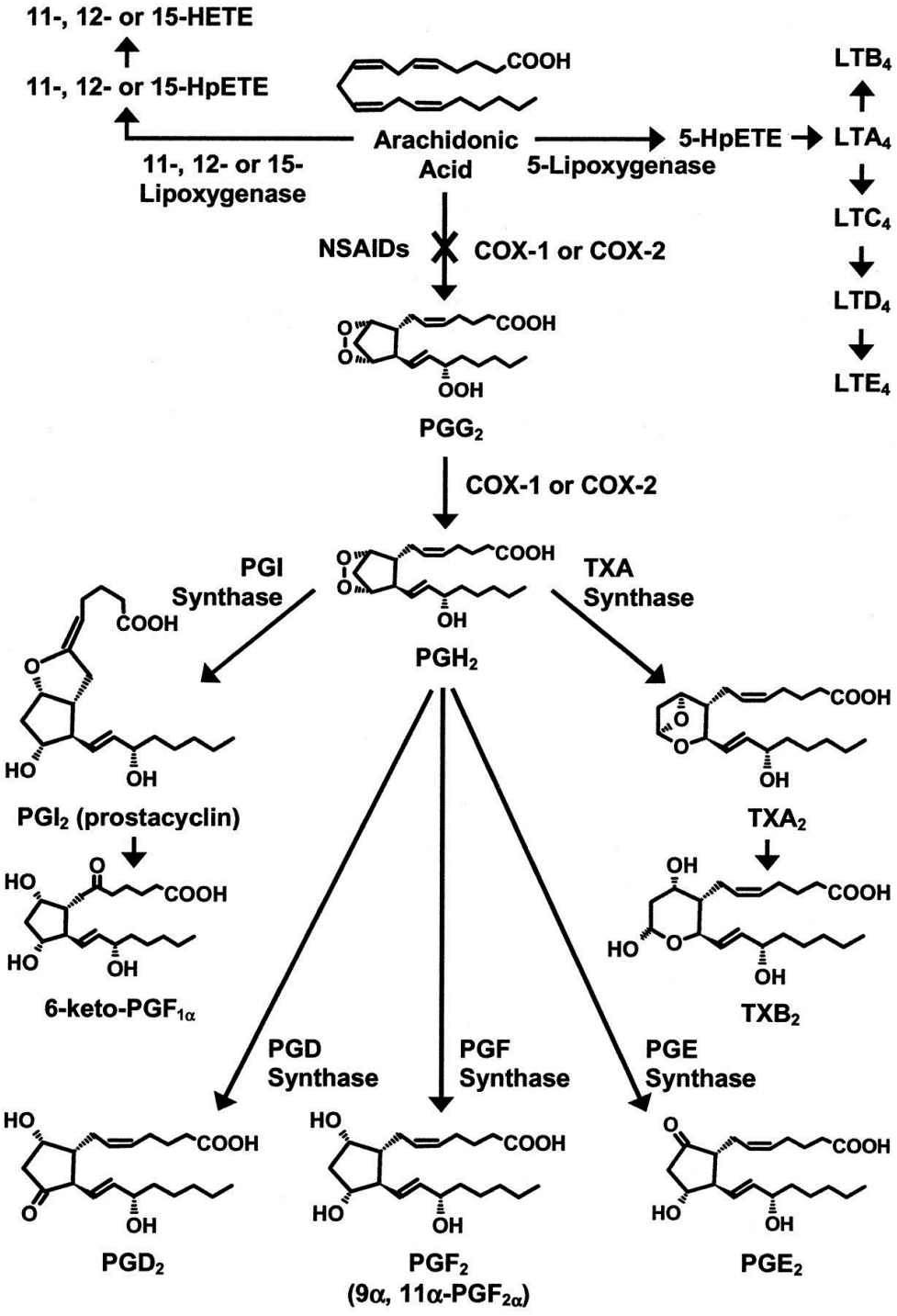

Figure 6: Schematic representing the pathways in which Arachidonic Acid is metabolized. AA can be metabolized into members of the leukotriene (LT) and the hydroxyeicosatetraenoic acid (HETE) family by the actions of lipoxygenases, and into the prostaglandin, prostacyclin (PGI), and thromboxane (TXA) family of metabolites by the actions of the cyclooxygenase enzymes in addition to the prostaglandin, prostacyclin, and thromboxane synthase enzymes. Retrieved from [74]

Fluctuations in prostaglandin levels has been discovered in many physiological and pathological states, including muscle exercise [75], ovulation [76], neuroinflammation, sleep promotion, modulation of synaptic plasticity [77], and most importantly, in the development of kidney damage [43]. The relationship between COX activity and kidney injury was studied, with focus on PGE_2 pathway, where it turned out that PGE_2 plays a role in fluid metabolism and blood pressure regulation in physiological conditions, but shifts to mediating kidney injury in pathological situations by binding to its G-protein-coupled receptors EP1, EP2, EP3, and EP4 [78]. It has also been shown that hyperfiltration, a symptom concurrent with the diabetic phenotype, leads to an increase in PGE_2 synthesis in an *in-vitro* model for fluid flow shear stress, as well as an increase in expression of COX-2 and EP_2 receptor [79]. Another study showed a short-lived increase in the p38 MAPK phosphorylation at short duration (10 minutes), and upregulated COX-2 expression at 4 hours in a PGE_2 induction model, with EP_4 knockouts, p38 MAPK, and AMPK knockouts abrogating the COX-2 upregulation, while blocking PKA had no effect on COX-2 expression [80]. This points at a positive feedback loop mechanisms existing for PGE_2, where its induction leads to the upregulation of the enzyme leading to its synthesis (COX-2).

The relationship the COX-2 inflammation pathway with the KKS has been studied in different systems before. In one study on a rat jejunum, it was shown that BK stimulates serosal afferent neurons by a direct action on the B2R and not on the B1R, and where the response of bradykinin is dependent on the presence of prostaglandins, and specifically PGE_2, where the stimulatory effect of BK is decreased to 55% of the control upon the introduction of a COX activity inhibitor naproxen [81]. Another study in the pleura of mice

showed that the activity of the BK agonist Tyr^{8}BK was inhibited with the addition of the selective COX-2 inhibitor NS-398 and the NSAID indomethacin [66]. One hallmark study showed that BK treatment of isolate coeliac, mesenteric, and extrapulmonary arteries induced the release of the prostaglandins, specifically PGE_2 and PGI_2. This study also suggested a correlation between the BK-induced prostaglandin release and the mechanical contraction of the blood vessels [82]. This sheds light on the linkage between COX and BK. However, it is yet to be demonstrated if these two molecules are linked in the podocyte signaling pathway.

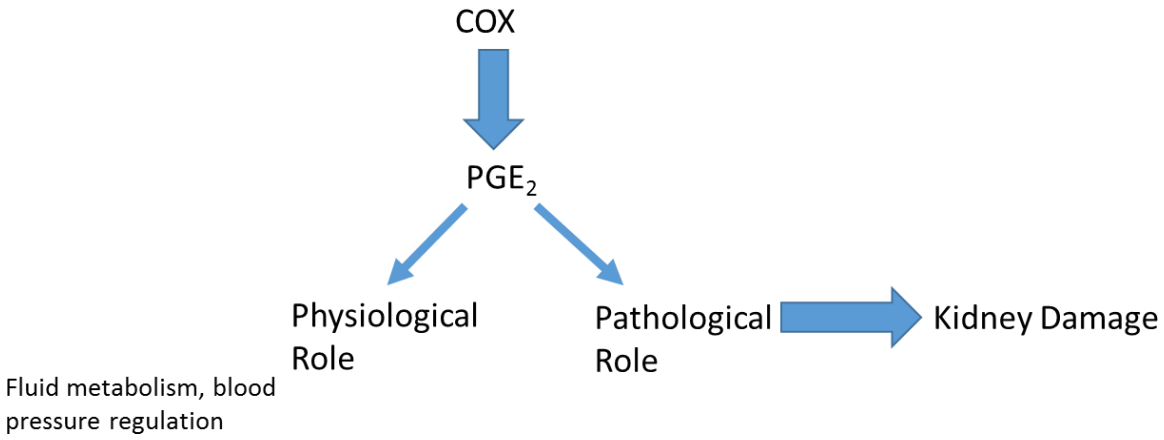

Figure 7: Schematic representing the suggested dual-roles of the COX/PGE_2 system in Physiological and Pathological conditions.

D. Proteomics:

Nowadays, adopting the proteomics approach for the discovery of novel biomarkers is becoming a widely-used analytical method in biomedical research. The advent of mass spectrometry has made possible the construction of the protein profile of a

cell at a given time and physiological/pathological state [83]. The pipeline of proteomic discovery of novel biomarkers goes as follows:

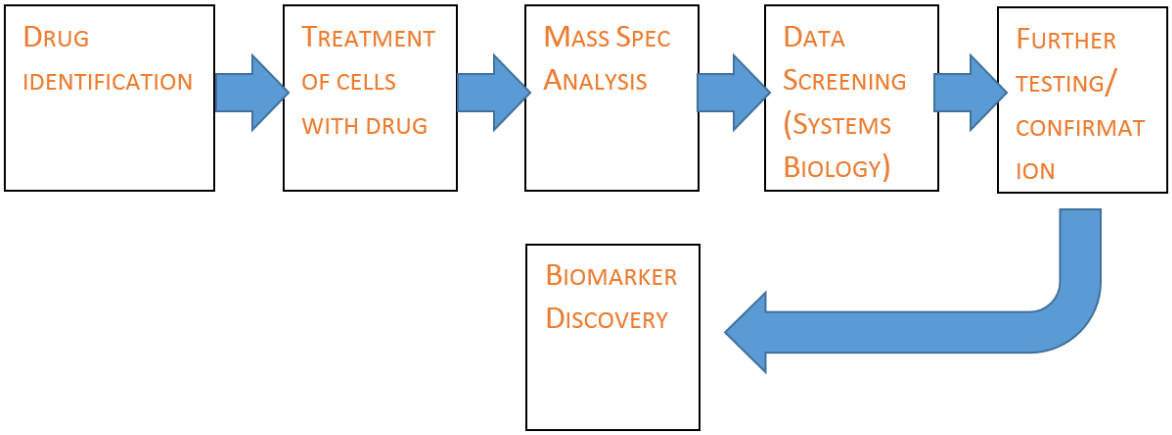

Figure 8: Schematic representing the pipeline of proteomic discovery of novel biomarkers, starting with the identification and isolation of the drug of interest, by the treatment of a target population of cells with said drug, performing mass spectrometry analysis on the cell lysate, obtaining the data and screening/filtering it from non-specific data, identifying prospective biomarkers, and finally by extensive testing on the suggested biomarkers, leading to biomarker discovery.

The first step in biomarker discovery is coming up with the drug whose effects on the target cells will be studied. Once the drug is decided, we proceed to treating the target cell population with said drug. Afterwards, mass spectrometry is performed on the cell lysates, and the data is collected. From the massive amount of raw data isolated, we need to filter the data to focus our study. Data is filtered according to the statistical significances of the observed proteins, and then systems biology is performed to link the observed protein changes to intracellular events, thus granting perspective of the cellular response after treatment with the drug. From the focused view acquired from the mass spectrometry and systems biology, we are able to look at certain molecules who have the highest chance of being correlated with the drug treatment. After extensive testing, potential biomarkers could be identified from this revised list of proteins.

E. Rationale/Aims:

Diabetic Nephropathy is the leading cause of end-stage renal disease, and is characterized by an increased albumin excretion rate, progressive renal damage, and eventually kidney failure [23]. Podocyte loss has been identified as a hallmark for the progression of diabetic nephropathy, where the loss of podocytes has been shown to be correlated with an increase in Albumin Excretion Rate (AER) [84]. The Kallikrein-Kinin system has been implicated in the progression of renal damage in multiple instances, where a study has shown that bradykinin is suggested to be involved in the altering of mesangial cell function through the actions of tubulin and MAPK [85], and multiple studies have demonstrated the renoprotective effect of knocking out the BK receptors [62,64,65,86,87] on the albumin excretion rate (AER) in the glomerulus. However, few studies have investigated the effect of BK treatment on podocytes as critical players in maintaining homeostatic kidney filtration.

In the present MS thesis, we aim to assess the protein profile of the cultured rat podocytes upon treatment with BK, and this was done by liquid chromatography/tandem mass spectrometry analysis. Next, we perform pathway enrichment analysis on the mass spectrometry data to broaden our understanding of the cellular processes occurring due to BK treatment. Many major pathways were discovered to be involved such as cell death and cytoskeletal activity. Analyzing and validating the data obtained by the LC-MS/MS and pathway enrichment analysis by western blotting and the enzyme immunoassay experiment

allowed us to elucidate the effect of BK treatment on the podocytes, and to identify key players in the signaling pathway of BK stimulation.

CHAPTER II

MATERIALS AND METHODS

A. Materials:

RPMI 1640, Insulin (I1882), Pen/Strep, Glutamine, Fetal Bovine Serum, Phosphate Buffer Saline, Bradykinin (SC090), Sodium Orthovanadate, Benzamidine, Sodium Pyrophosphate, Sodium Fluoride, β-mercaptoethanol Acrylamide, Bis-acrylamide, Sodium Dodecyl Sulfate, Methanol, Tween-20, and Trichloroacetic acid (TCA) were purchased from Sigma-Aldrich (St Louid, Missouri, United States). DC Protein™ assay, Bovine Serum Albumin, Tris, Glycine, TEMED, and Clarity™ Western Ecl were purchased from Biorad (Hercules, California, United States). HEPES, Bromophenol Blue, Ponceau Red, and PMSF were purchased from Amresco (daughter of VWR Funding Inc, West Chester, Pennsylvania, United States). PD 98059 and Ibuprofen were purchased from Bertin Pharma (78180 Montigny le Bertonneux, France). Aprotinin and Leupeptin were purchased from Roche (Basel, Switzerland). Antibodies: Anti-Actin (Abcam, ab8227), Anti-CTGF (Abcam, ab6992), anti- Nephrin antibody Y17-R (Abcam, ab136894), monoclonal antibody selective to COX-2 (clone CX 214 from Dr. Aida Habib, described in [88]), Phospho-p44/42 MAPK (ERK1/2) rabbit mAb (Cell Signaling, 4370s), p44/42 MAPK rabbit mAb (ERK1/2) (Cell Signaling, 4695s), Peroxidase-conjugated AffiniPure Donkey Anti-Rabbit IgG (H+L) (Jackson Immunoresearch, 711-035-152), Peroxidase-conjugated AffiniPure Donkey Anti-Mouse IgG (H+L) se (Jackson Immune, 715-035-150)

B. Cell Culture:

The rat podocytes used were originally isolated by Kreisberg et al at the Department of Pathology at Harvard Medical School in 1978 [89]. The basic media was prepared from Sigma-Aldritch's RPMI 1640 powder, with the complete media having insulin, PS, Glutamine, FBS, and HEPES. The starvation media included all these components minus the Fetal Bovine Serum and Insulin. The podocytes were sub-cultured once every 4 days. The podocytes were seeded in 6-well plates for treatment, and the seeding density was 120,000 cells/well. The plated podocytes were left in their complete media for 2 days, then were starved with the RPMI 1640 starvation media for a day, and then had their starvation media changed 2 hours prior to the introduction of the drugs. BK was introduced at a concentration of 10^{-7} M. This concentration is used because dose-effect studies of BK concentration show a at 10^{-7} M. Ibuprofen at 10^{-6} M was introduced 1 hour before the addition of BK, and PD-98059 at 25μM was introduced 30 minutes before BK treatment. When the treatments were done, 1mL of the media was collected for PGE_2 measurement for PGE_2 release assay. The rest of the media is aspirated, and the wells are washed twice with PBS with Ca^{2+}/Mg^{2+}. Finally, the plates are frozen at -20º C until they are ready to be treated with lysis buffer for protein extraction.

C. Mass Spectrometry

1. Extraction and tryptic digestion of proteins

Cells were homogenized using VWR® Disposable Pellet Mixers (VWR International, Radnor, PA) in 500-μL extraction buffer (5M urea, 40mM Tris, 0.2%w/v CHAPS). Next, the samples were sonicated for 1 hour at 4°C prior to centrifugation for 45

min at 15,000 G with the centrifuge held at 4°C. The supernatant was then collected in separate containers. The buffer of the extracted protein was exchanged into 50 mM ammonium bicarbonate using 5kDa MWCO spin concentrators (Agilent Technologies, Santa Clara, CA). This buffer is needed for efficient tryptic digestion.

A 10-µg aliquot of each sample, determined by BCA protein assay (Thermo Scientific/Pierce, Rockford, IL), was diluted to 20 µL by 50 mM ammonium bicarbonate. Thermal denaturation was performed at 65º C for 10 min. A 0.75-µL aliquot of 200mM DTT was added to reduce the sample at 60º C for 45 min. A 3 µL aliquot of 200mM IAA was added to alkylate the sample at 37.5º C for 45 min in the dark. Excess IAA was consumed by the addition of another 0.75 µL aliquot of 200mM DTT and incubation at 37.5º C for 30 min. The tryptic digestion was performed at 37.5º C for 18 hours followed by microwave digestion at 45º C and 50W for 30min. A 0.5 µL aliquot of neat formic acid was added to quench the digestion. Finally, a 3 µL aliquot of 5 ng/µL reduced and permethylated dextran was added to each sample as internal standard to offset any potential injection variance.

2. Liquid Chromatography - Tandem mass spectrometry (LC-MS/MS) assay

LC-MS/MS was acquired using Dionex 3000 Ultimate nano-LC system (Dionex, Sunnyvale, CA) interfaced to LTQ Orbitrap Velos and TSQ Vantage mass spectrometers (Thermo Scientific, San Jose, CA) equipped with nano-ESI source. The separation was attained using Acclaim PepMap RSLC columns (75 µm I.D. x 15 cm, 2 µm particle sizes, 100 Å pore sizes) (Dionex, Sunnyvale, CA) with a flow rate of 350 nL/min. The column compartment was maintained at 29.5º C. The LC elution gradient of solvent B used in both

LC-MS/MS analysis was: 5% over 10 min, 5%-20% over 55 min, 20-30% over 25 min, 30-50% over 20 min, 50%-80% over 1 min, 80% over 4 min, 80%-5% over 1 min and 5% over 4 min. Solvent B consisted of 100% ACN with 0.1% formic acid while solvent A composed of 2% ACN with 0.1% formic acid.

The LTQ Orbitrap Velos mass spectrometer was operated in positive mode with the ESI voltage set to 1500V. Data dependent acquisition mode was employed to achieve two scan events. The first scan event was a full MS scan of 380-2000 m/z at a mass resolution of 15,000. The second scan event was CID MS/MS of parent ions selected from the first scan event with an isolation width of 3.0 m/z, at a normalized collision energy (CE) of 35%, and an activation Q value of 0.250. The CID MS/MS scans were performed on the 30 most intense ions observed in the MS scan event. The dynamic exclusion was set to have repeat count of 2, repeat duration of 30s, exclusion list size 200 and exclusion duration of 90s.

The TSQ Vantage mass spectrometer was operated in positive mode with an ESI voltage of 1800V. Data independent acquisition mode was used for the MRM experiments. Predefined precursor and transition ions were monitored to select specific targeted peptides corresponding to each candidate protein with 10.0 sec chromatogram filter peak width. The MRM experiments were performed at a cycle time of 2.000 sec and a Q1 peak width of 0.70 min for 400-1500 m/z mass range. The normalized collision energy value was 30% with a collision gas pressure of 1.5 mTorr in Q2.

3. LC-MS/MS data analysis

Liquid chromatography-electrospray ionization-tandem mass spectrometry (LC-ESI-MS/MS) data was used to generate mascot generic format file (*.mgf) by Proteome Discover version 1.2 software (Thermo Scientific, San Jose, CA) then searched using SwissProt database (Rattus) in MASCOT version 2.4 (Matrix Science Inc., Boston, MA). Iodoacetamide modification of cysteine was set as a fixed modification, while oxidation of methionine was set as a variable modification. An m/z tolerance of 5 ppm was set for the identification of peptides with maximum 2 missed cleavages. Also, tandem MS ion tolerance was set within 0.8 Da with label-free quantification. Scaffold Q+ (Proteome Software, Portland, OR) was employed for spectral counts quantitation. Proteins shown significant difference ($p<0.05$, unpaired student t-test) in spectral counts quantitation results were confirmed by MRM LC-MS/MS experiment. Each sample was injected three times to make a technical triplicate of MRM experiment. The most intense 1 or 2 peptides corresponding to each candidate protein were selected as target peptides. The three transitions of each target peptide were suggested by Pinpoint (Thermo Scientific, San Jose, CA). The MRM experiment results were investigated using Pinpoint. Peak area of each target peptide was normalized by the peak area of the glycan with 4 glucose units (m/z= 896.507). The normalized intensity of target peptides corresponding to each candidate protein were summed up to represent the abundance of the certain protein. A t-test ($\alpha=0.05$) was performed to evaluate the statistical significance.

4. Systems Biology

Ingenuity Pathway Analysis software (Ingenuity® Systems) and Pathway Studio (Ariadne Genomics) were employed to examine functional correlations within the different treatment groups. Data sets containing protein identifiers (Uniprot-KB) and corresponding expression values were uploaded into the application. Each protein identifier was mapped to its corresponding protein object in the Ingenuity Pathways Knowledge Base in the case of IPA, and to the Pathway Studio knowledgebase in the case of Pathway Studio. All mapped proteins were differentially expressed with $p < 0.01$ and overlaid onto global molecular networks developed from information contained in the knowledge base. Networks were then algorithmically generated based on their connectivity.

D. Protein Assay

1. Extraction and Quantification:

The frozen plates of treated podocytes were collected, and 200 μL of the lysis buffer (made with a RIPA base and with the inhibitors Leupeptin 2μg/ml, Aprotinin 2 μg/ml, Sodium Orthovanadate 2 mM, PMSF 1 mM, Benzamidine 1 mM, Sodium Pyrophosphate 1 mM, and Sodium Fluoride 10 mM) was added to each well and left for 10 minutes on ice. Following that, the cells were scraped with a plastic scraper and the cell lysate was collected and centrifuged at 13,800 G and 4º C for 10 minutes. The supernatant containing the proteins was then collected and transferred into a labeled eppendorf.

The proteins were quantified using the Lowry assay. The standard curve was constructed using known concentrations of Bovine Serum Albumin. 5 μL of the protein samples mixed with 5 μL of double-distilled H_2O and placed in a 96-well plate, where 25

μL of Lowry Solution A+S (Ratio is 20 μL of solution S for every 1000 μL solution A) and 200 μL of Lowry Solution B were added for quantification. The samples were read on a spectrophotometer at 750 nm wavelength and then compared to the standard BSA curve to determine the total protein concentration. The necessary calculations were then performed to achieve equal loading of total proteins, giving us 30 μL of protein + double-distilled H_2O, and 10 μL of the lamellae buffer for migration. At this point, the proteins were ready for loading and migration.

2. Migration and Transfer:

20-30 μg of proteins with ddH_2O in 30 μL and 10 μL of Laemmli buffer were ran on SDS-PAGE 8% and 10% gels were composed of bis-acrylamide, Tris (pH 8.8, 0.39M for resolving gel, pH 6.8, 0.13M for stacking gel), Sodium Dodecyl Sulfate 0.1%, Ammonium Per-sulfate 0.1%, and TEMED 0.04%. Migration was carried out in a 1x migration buffer (0.05 M Tris, 0.384 M glycine, 0.035 SDS), then the membranes were transferred to a nitrocellulose membrane in 1x transfer buffer (0.025 M Tris, 0.192 M Glycine, 20% Methanol, 0.01% SDS). Membranes were then blocked in 5% milk in 1x TBST (0.025 M Tris, 0.15 mM NaCl, 2 mM Kcl, 1% Tween, pH 7.4).

3. Western Blotting:

Immunoblotting was performed using several primary antibodies (mentioned in the Materials section), followed by serial washing steps in 1x TBST. Membranes are then incubated with the secondary antibody for 1 hours, followed by another set of serial washing steps in 1x TBST. Membranes were then activated with the Biorad ECL kit and

visualized on the BIORAD ChemiDoc MP imaging System. Bands were quantified using ImageJ software, and compared to housekeeping genes for loading control.

E. Metabolite Assay

Immunoenzyme analysis of PGE_2 was performed according to the protocol mentioned in [90].

F. Statistical Analysis

Each experiment was performed at least in triplicate. Data are expressed as mean ± SE and corresponding statistical significance being analyzed by Prism GraphPad software. The differences in the mean between groups were analyzed by student t-test for two tailed unpaired analysis. Significance was considered if $p<0.05$.

CHAPTER III

RESULTS:

A. Investigation of our Proteomic Data:

The experimental groups were: podocytes treated with BK for 3 hours, podocytes treated with BK for 6 hours, and control podocytes. Triplicates of the experimental groups were sent for mass spectrometry analysis. The variation of mass spectrometry performed is Liquid Chromatography- Tandem Mass Spec (LC-MS/MS). LC-MS/MS analysis showed a regulation of 281 proteins. This number was reduced to 61 proteins when searching for significance (p value < 0.05), split among 3 groups that compare the protein profile between each timepoint of treatment, resulting in the groups “Control vs 3 hours BK treatment”, “Control vs 6 hours BK treatment”, and “3 hours vs 6 hours BK treatment”. The pattern of protein upregulation and downregulation in the 3 experimental groups is shown in the following table.

Table 1: Table showing the variation of the regulated protein numbers in the 3 experimental groups

Condition	# of proteins upregulated	# of proteins downregulated
Ctr vs 3 hours	6	7
Ctr vs 6 hours	9	25
3 hours vs 6 hours	12	22

The proteins with a p-value higher than 0.05 are listed in the following tables along with their accession number, protein symbol, fold change, and Log2 fold change.

Table 2: Comparative list of proteins in the BK-stimulated podocytes for 3 hours compared to control.

Accession	Protein Name	Symbol	p-value	Fold change	Log2 Fold change
P16638	ATP Citrate Lyase	ACLY	0.049	0.149	-2.748
P11240	Cytochrome c oxidase subunit 5A	COX5A	0.031	5.344	2.418
P31977	Ezrin	EZR	0.033	1.358	0.442
P63095	GNAS Complex locus	GNAS	0.034	1.318	0.399
P27008	Poly(ADP-ribose) polymerase 1	PARP1	0.018	1765.722	10.786
P85125	Polymerase I and transcript release factor release factor	PTRF	0.021	0.662	-0.596
P49432	Pyruvate dehydrogenase	PDHB	0.037	0.376	-1.409
P61589	Ras homolog family member A	RHOA	0.047	0.507	-0.981
P63245	Receptor for activated C Kinase1	RACK1	0.044	0.306	-1.707
P62282	Ribosomal Protein S11	RPS11	0.042	0.186	-2.424
P29314	Ribosomal Protein S9	RPS9	0.002	1.844	0.883
P16036	Solute carrier family 25	SLC25A3	0.003	2.562	1.357
Q5I0E7	Transmembrane p24 trafficking protein 9	TMED9	0.014	0.104	-3.262

Table 3: Comparative list of proteins in the BK-stimulated podocytes for 6 hours compared to control.

Accession	Protein Name	Symbol	p-value	Fold change	Log2 Fold change
P60711	Actin Beta	ACTB	0.043	2.159	1.111
Q9Z1P2	Actinin alpha 1	ACTN1	0.008	1.959	0.970
Q64057	Aldehyde Dehydrogenase 7 family member A1	ALDH7A1	0.040	3.771	1.915

P07150	Annexin A1	ANXA1	0.004	2.013	1.009
Q9JM53	Apoptosis inducing factor, mitochondrial	AIFM1	0.016	0.001	-10.751
P40329	arginyl-tRNA synthetase (RARS)	RARS	0.015	2.237	1.161
A1L108	Actin-related protein 2/3 complex subunit 5-like protein	ARPC5L	0.042	0.186	-2.425
Q9WU82	Catenin Beta 1	CTNNB1	0.009	0.171	-2.545
P62634	CCHC-type zinc finger nucleic acid binding protein	CNBP	0.024	0.198	-2.339
Q8VHF5	Citrate Synthase	CS	0.009	5.960	2.575
O35142	Coatomer protein complex subunit beta 2	COPB2	0.017	0.101	-3.308
P00173	Cytochrome b5 Type A	CYB5A	0.008	0.082	-3.609
Q62638	Golgi glycoprotein 1	GLG1	0.026	0.346	-1.531
Q3ZU82	Golgin 5A	GOLGA5	0.042	0.001	-10.961
P63159	High mobility group box 1	Hmgb1	0.009	0.112	-3.159
Q00715	Histone Cluster 1, H2bl	-	0.039	0.721	-0.471
Q63617	Hypoxia up-regulated 1	HYOU1	0.027	1.539	0.622
P49134	Integrin subunit Beta 1	ITGB1	0.014	0.152	-2.713
P70615	Lamin B1	LMNB1	0.038	0.312	-1.681
P85125	Polymerase I and transcript release factor release factor	PTRF	0.002	0.297	-1.750
Q63009	Protein arginine methyltransferase 1	PRMT1	0.020	4.450	2.154
P62138	Protein Phosphatase 1	PPP1CA	0.001	3.394	1.763
O35509	RAB11B, member RAS oncogene family	RAB11B	0.046	0.454	-1.138
Q6NYB7	RAB1A, member RAS oncogene family	RAB1A	0.015	0.314	-1.670
P62828	RAN, member RAS oncogene family	RAN	0.045	0.224	-2.161
Q9JK11	Reticulon 4	RTN4	0.018	0.497	-1.007
Q27W01	RNA binding motif protein 8A	RBM8A	0.008	0.001	-10.174
Q62991	Sec 1 family domain	SCFD1	0.006	0.000	-11.026
Q09073	Solute carrier family 25	SLC25A5	0.003	0.608	-0.717
Q5I0E7	Transmembrane p24 trafficking protein 9	TMED9	0.006	0.000	-11.362

Q6P9T8	Tubulin Beta 4B class Ivb	TUBB4B	0.007	0.783	-0.353
P69897	Tubulin Beta class I	TUBB	0.020	0.895	-0.160
P85972	Vinculin	VCL	0.028	0.242	-2.049
Q9Z2L0	Voltage dependant anion channel 1	VDAC1	0.019	0.409	-1.289

Table 4: Comparative list of proteins in the BK-stimulated podocytes for 3 hours compared to BK-stimulated podocytes for 6 hours.

Accession	Protein Name	Symbol	p-value	Fold change	Log2 Fold change
P60711	Actin Beta	ACTB	0.020	2.608	1.383
Q9Z1P2	Actinin alpha 1	ACTN1	0.014	1.698	0.764
Q63151	acyl-CoA synthetase long-chain family member 3	ACSL3	0.044	0.246	-2.025
Q64057	Aldehyde Dehydrogenase 7 family member A1	ALDH7A1	0.035	3.099	1.632
P07150	Annexin A1	ANXA1	0.027	1.572	0.652
Q8VHF5	Citrate Synthase	CS	0.020	2.966	1.569
O35142	Coatomer protein complex subunit beta 2	COPB2	0.008	0.139	-2.851
Q5U2X6	Coiled-coil domain containing 47	CCDC47	0.029	0.000	-11.177
Q64654	Cytochrome P450 family 51 subfamily A member 1	CYP51A1	0.045	0.203	-2.297
Q9Z1X1	Extended synaptotagmin 1	ESYT1	0.016	0.177	-2.494
P35571	Glycerol-3-phosphate dehydrogenase 2	GPD2	0.041	0.000	-11.906
P63095	GNAS Complex locus	GNAS	0.004	0.615	-0.700
P82995	hsp90 alpha family class A member 1	HSP90AA1	0.004	2.293	1.197
P34058	hsp90 alpha family class B member 1	HSP90AB1	0.044	2.382	1.252
P49134	Integrin subunit Beta 1	ITGB1	0.009	0.120	-3.055
P70615	Lamin B1	LMNB1	0.042	0.325	-1.623

P85125	Polymerase I and transcript release factor release factor	PTRF	0.007	0.449	-1.154
Q5XIH7	Prohibitin 2	PHB2	0.035	0.494	-1.018
P35355	Prostaglandin-endoperoxide synthase 2	PTGS2	0.016	1.666	0.737
Q63009	Protein arginine methyltransferase 1	PRMT1	0.007	15.617	3.965
P62138	Protein Phosphatase 1	PPP1CA	0.015	2.926	1.549
Q6NYB7	RAB1A, member RAS oncogene family	RAB1A	0.011	0.268	-1.899
P62828	RAN, member RAS oncogene family	RAN	0.038	0.198	-2.334
Q9JK11	Reticulon 4	RTN4	0.018	0.473	-1.080
P04644	Ribosomal protein S17	RPS17	0.047	0.219	-2.191
P62083	Ribosomal protein S7	RPS7	0.006	0.000	-12.192
Q62991	Sec 1 family domain	SCFD1	0.008	0.001	-10.543
Q09073	Solute carrier family 25	SLC25A5	0.048	0.621	-0.687
Q9QWN8	Spectrin Beta, non-erythrocytic 2	SPTBN2	0.018	2.452	1.294
P28480	T-complex 1	TCP1	0.047	6.174	2.626
Q62733	Thymopoietin	TMPO	0.039	0.223	-2.167
Q75Q39	Translocase of outer mitochondrial membrane 70	TOMM70	0.020	0.108	-3.217
Q66HG5	Transmemberane 9 superfamily member 2	TM9SF2	0.044	0.605	-0.726
Q9Z2L0	Voltage dependant anion channel 1	VDAC1	0.013	0.317	-1.656

B. Investigation of the Comparative Protein Expression by Venn diagram:

To facilitate the analysis of the different proteins expressed in the different groups, we construct a Venn diagram containing the hits from the mass spectrometry analysis. The ensuing tables list the grouped proteins.

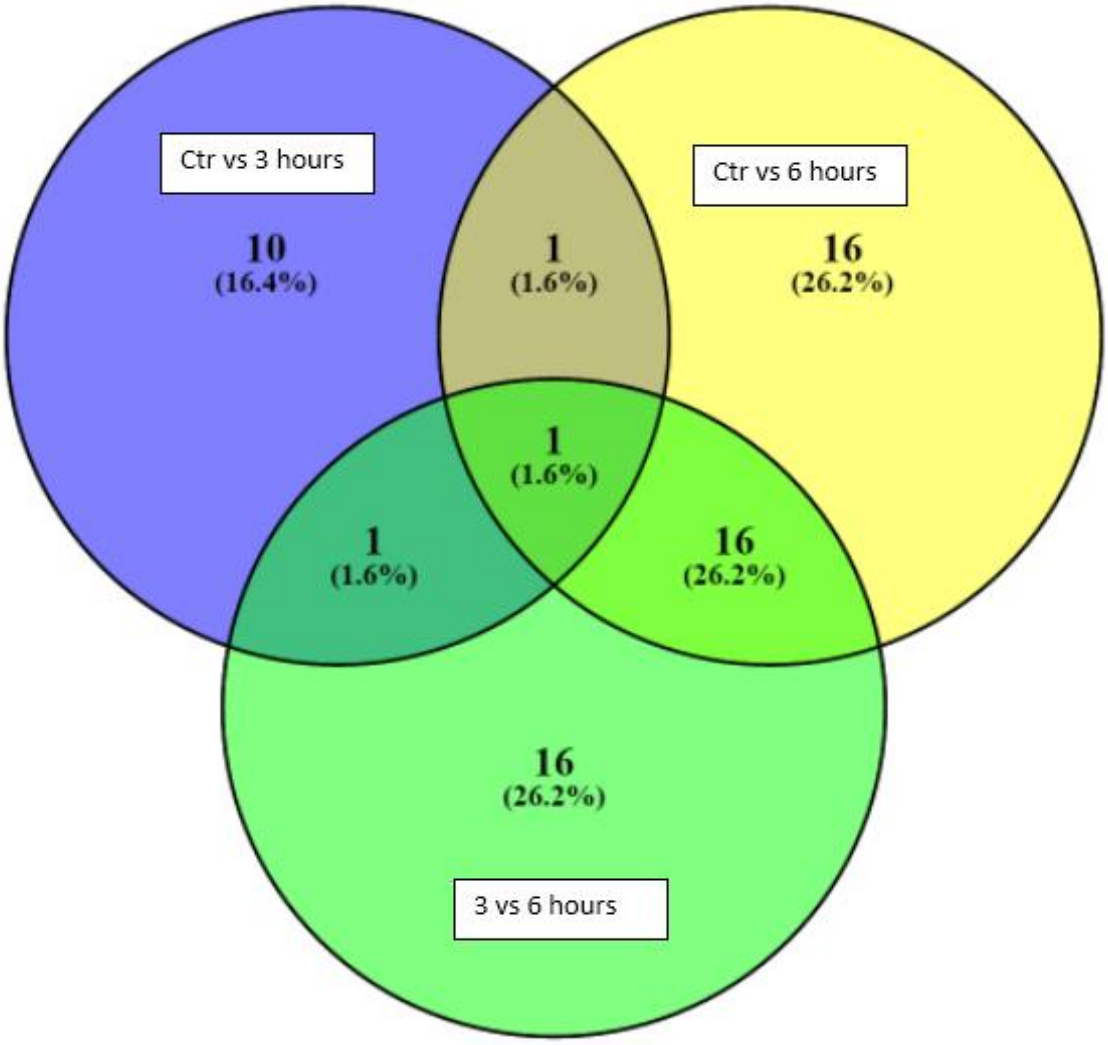

Figure 9: Venn diagram showing the appearance of common proteins between the three experiments of BK-treated podocytes for 3 hours versus controls, BK-treated podocytes for 6 hours versus controls, and BK-treated podocytes for 3 hours versus BK-treated podocytes.

Table 5: List of proteins according to their appearance in the different experimental groups of the mass spectrometry

Common between all experiments: Polymerase I and transcript release factor release factor
Common between "Ctr vs 3 hours" and "Ctr vs 6 hours": Transmembrane p24 trafficking protein 9
Common between "Ctr vs 3 hours" and "3 vs 6 hours":

GNAS Complex locus
Common between "Ctr vs 6 hours" and "3 vs 6 hours": Protein Phosphatase 1 Solute carrier family 25 Annexin A1 Sec 1 family domain Actinin alpha 1 Citrate Synthase Integrin subunit Beta 1 RAB1A COPB2 Reticulon 4 Voltage dependant anion channel 1 Protein arginine methyltransferase 1 Lamin B1 Aldehyde Dehydrogenase 7 family member A1 Beta Actin RAN
Unique to "Ctr vs 3 hours": Ribosomal Protein S9 Solute carrier family 25 (1) PARP1 COX5A Ezrin Pyruvate dehydrogenase Ribosomal Protein S11 Receptor for activated C Kinase1 RHOA ATP Citrate Lyase
Unique to "Ctr vs 6 hours": Tubulin Beta 4B class Ivb Cytochrome b5 Type A RNA binding motif protein 8A Catenin Beta 1 High mobility group box 1 arginyl-tRNA synthetase (RARS) Apoptosis inducing factor, mitochondrial Tubulin Beta class I CCHC-type zinc finger nucleic acid binding protein Golgi glyoprotein 1

Hypoxia up-regulated 1 Vinculin Histone Cluster 1, H2bl Golgin 5A Arp 2/3 RAB 11B
Unique to "3 vs 6 hours": hsp90 alpha family class A member 1 Ribosomal protein S7 Extended synaptotagmin 1 Cyclooxygenase-2 (COX-2) Spectrin Beta, non-erythrocytic 2 TOMM70 Coiled-coil domain containing 47 Prohibitin 2 Thymopoietin Glycerol-3-phosphate dehydrogenase 2 Transmemberane 9 superfamily member 2 hsp90 alpha family class B member 1 acyl-CoA synthetase long-chain family member 3 Cytochrome P450 family 51 subfamily A member 1 T-complex 1 Ribosomal protein S17

Furthermore, we took the most relevant proteins (according to number of links) and shifted them to the middle of the display.

From the list of modulated proteins, few proteins of particular interest stick out Those proteins were RhoA from the Control versus 3 hours of BK treatment experiment, β-Catenin, Integrin-β1, and β-Actin from the Control versus 6 hours of BK treatment experiment, and PTGS-2 (COX-2) from the 3 hours of BK treatment versus 6 hours of BK treatment experiment. We will discuss each of these proteins along with their relevance to diabetic nephropathy in the discussion segment of this thesis.

C. Clustering of the Expressed proteins via heatmap:

From the mass spectrometry data, heatmaps were constructed for the 3 experimental groups showing the clustering of modulated proteins, where a row represents a protein and a column represents one of the triplicates for each experimental group.

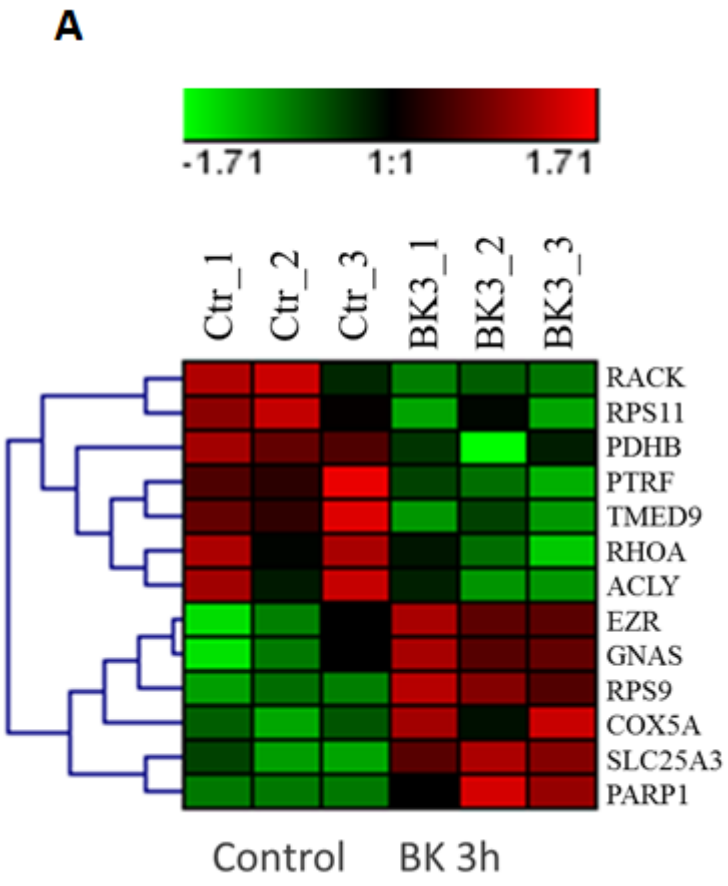

B

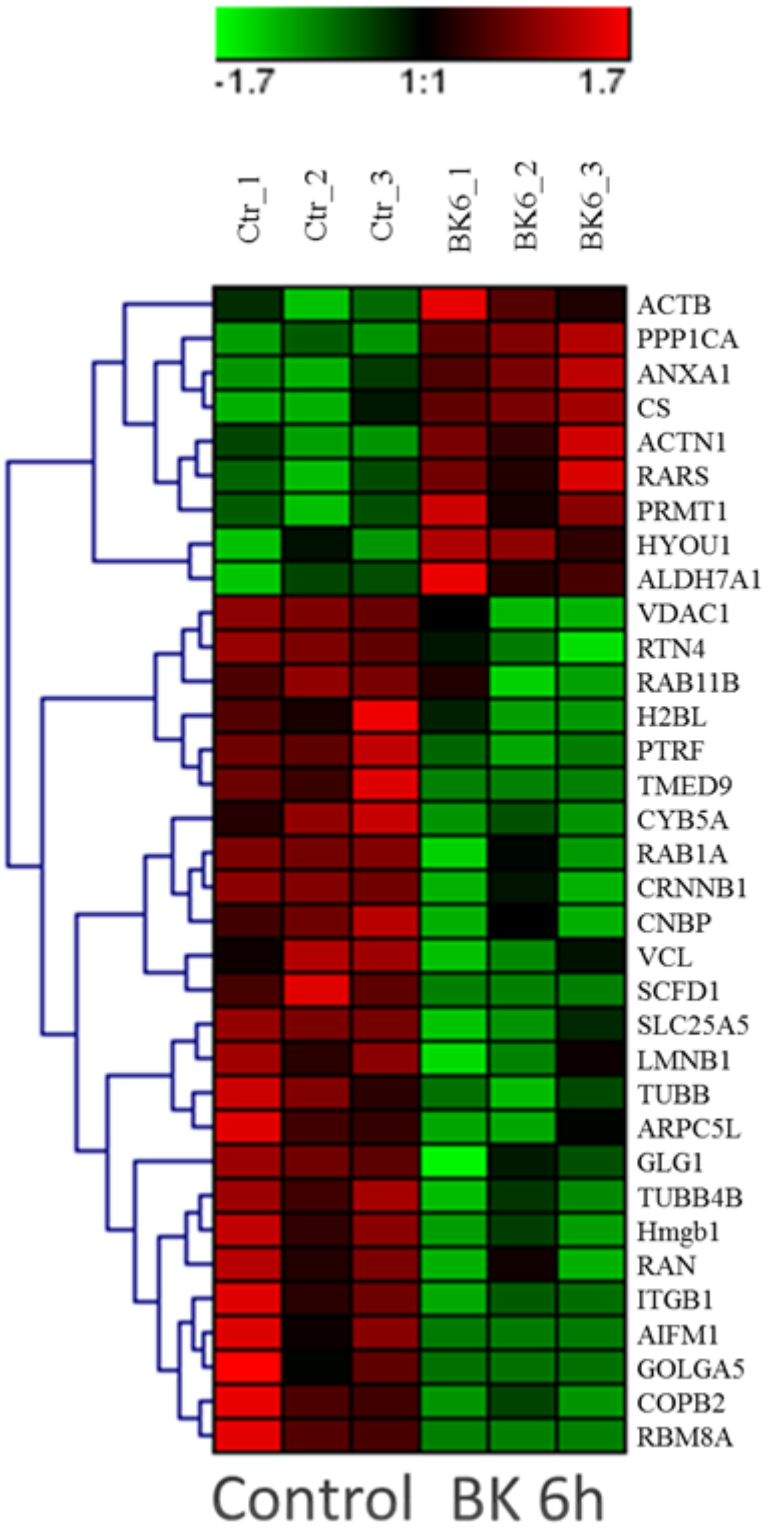
-1.7
1:1
1.7
Ctr_1
Ctr_2
Ctr_3
BK6_1
BK6_2
BK6_3
ACTB
PPP1CA
ANXA1
CS
ACTN1
RARS
PRMT1
HYOU1
ALDH7A1
VDAC1
RTN4
RAB11B
H2BL
PTRF
TMED9
CYB5A
RAB1A
CRNNB1
CNBP
VCL
SCFD1
SLC25A5
LMNB1
TUBB
ARPC5L
GLG1
TUBB4B
Hmgb1
RAN
ITGB1
AIFM1
GOLGA5
COPB2
RBM8A
Control
BK 6h

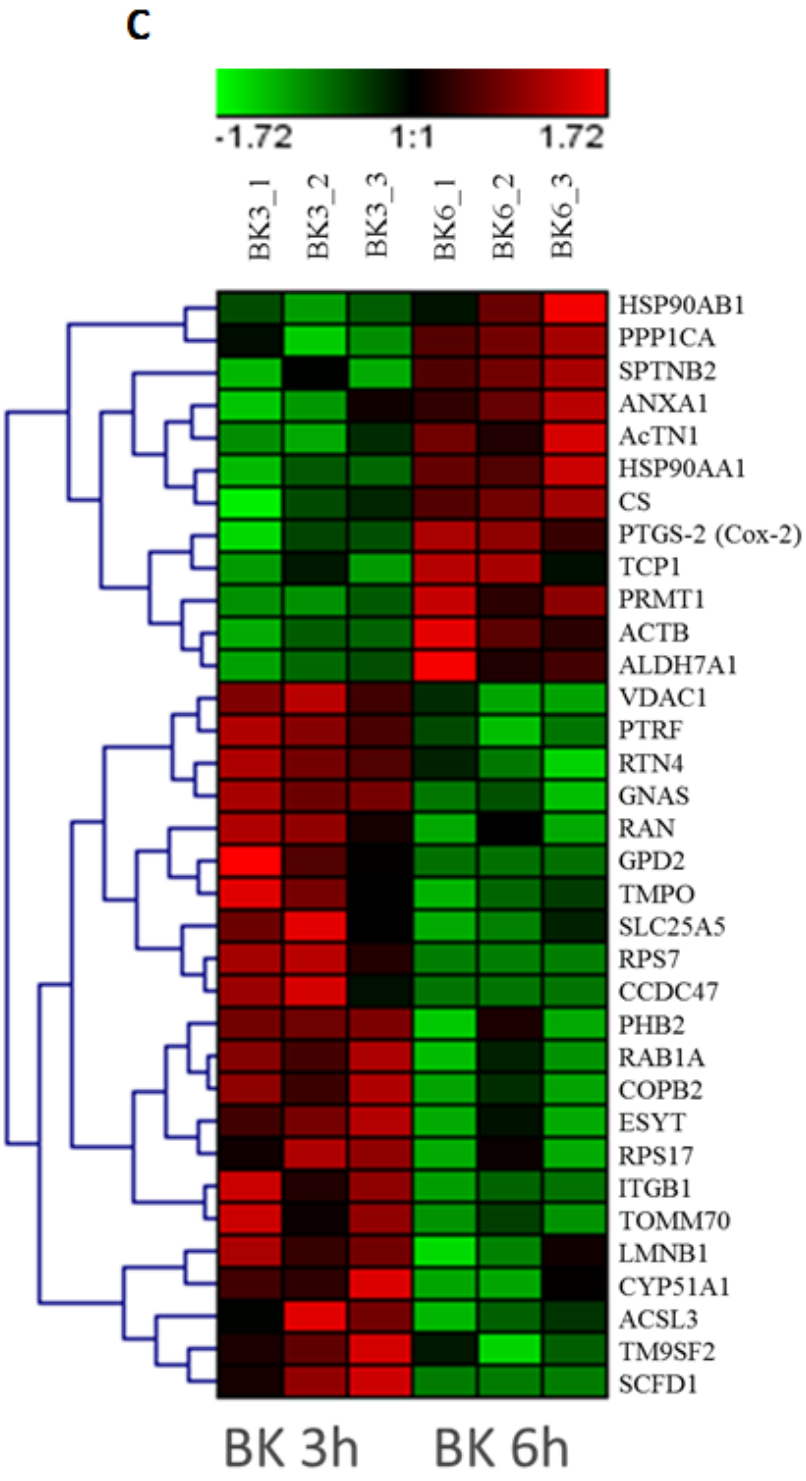

Figure 10: Heatmap showing the different proteins expressed in the 3 experimental groups: Control vs 3 hours BK treatment (Figure A), Control vs 6 hours BK treatment (Figure B), and 3 hours vs 6 hours BK treatment (Figure C). Each row represents a different protein while each column represent one triplicate from the corresponding experimental group.

D. Construction of Protein Pathways:

Following the mass spectrometry analysis, we construct pathways using Pathway Studio, linking expressed proteins to other expressed proteins, manually inputted proteins (based on relevance in literature) and cell processes and diseases. The software constructs links between the proteins and cellular states with the thickness of the arrow corresponding to the strength of the link between the proteins based on the number of publications in the software's knowledgebase supporting this link. Figure 11shows the constructed pathways for each individual experimental group. Suggested proteins were only kept if they were confirmed to be linked by the software to at least one of our proteins, and were highlighted in yellow to avoid confusion with expressed proteins. The proteins found at the center of the pathways were the proteins deemed to be "of interest" from the mass spectrometry data. These proteins are shown to have extensive links with the other expressed and suggested proteins as well as being linked to the cell processes and diseases.

A

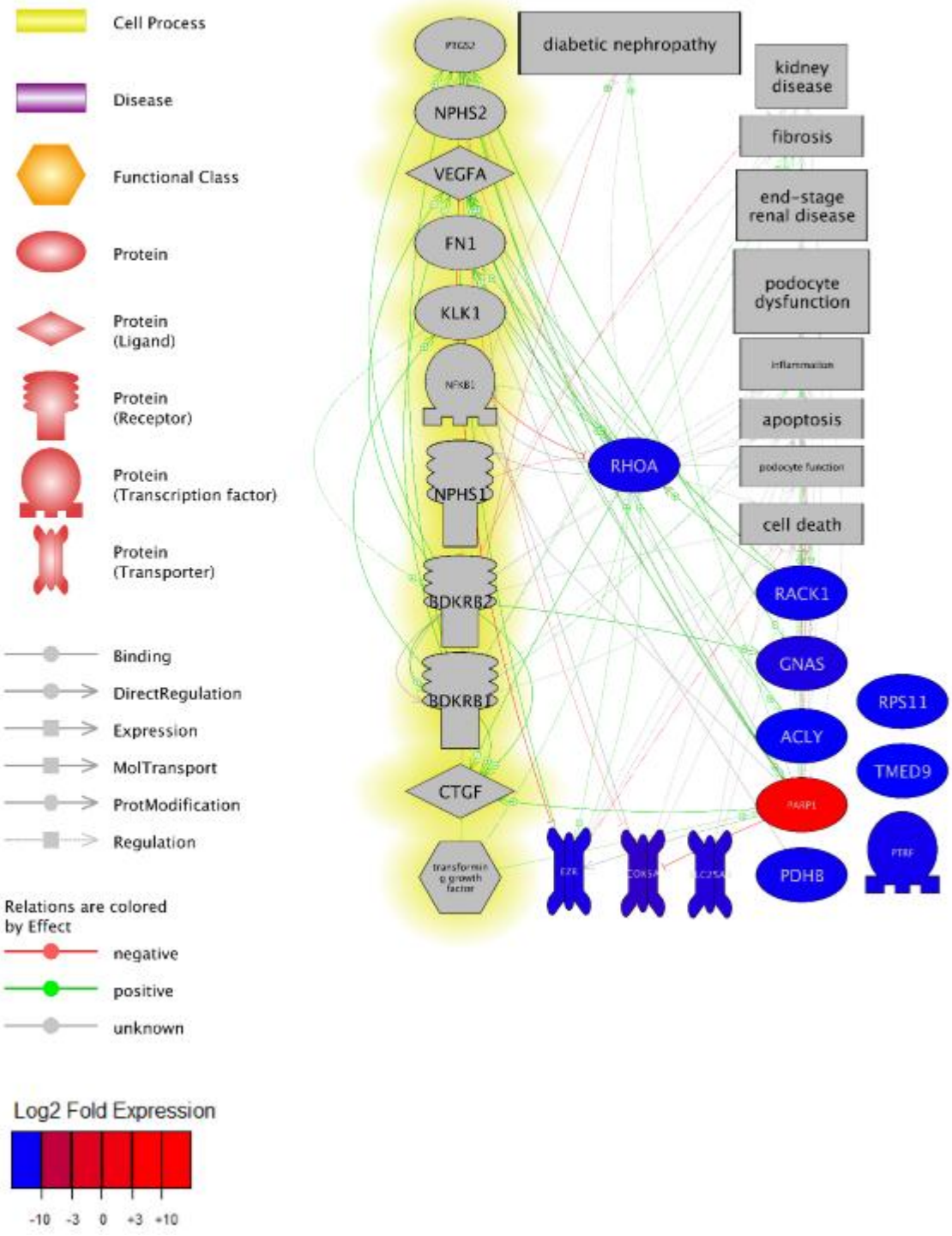
Cell Process
Disease
Functional Class
Protein
Protein (Ligand)
Protein (Receptor)
Protein (Transcription factor)
Protein (Transporter)
Binding
DirectRegulation
Expression
MolTransport
ProtModification
Regulation
Relations are colored by Effect
negative
positive
unknown
Log2 Fold Expression
-10 -3 0 +3 +10
diabetic nephropathy
kidney disease
fibrosis
end-stage renal disease
podocyte dysfunction
inflammation
apoptosis
podocyte function
cell death
NPHS2
VEGFA
FN1
KLK1
NPHS1
BDKRB2
BDKRB1
CTGF
RHOA
RACK1
GNAS
ACLY
PARP1
PDHB
RPS11
TMED9

B

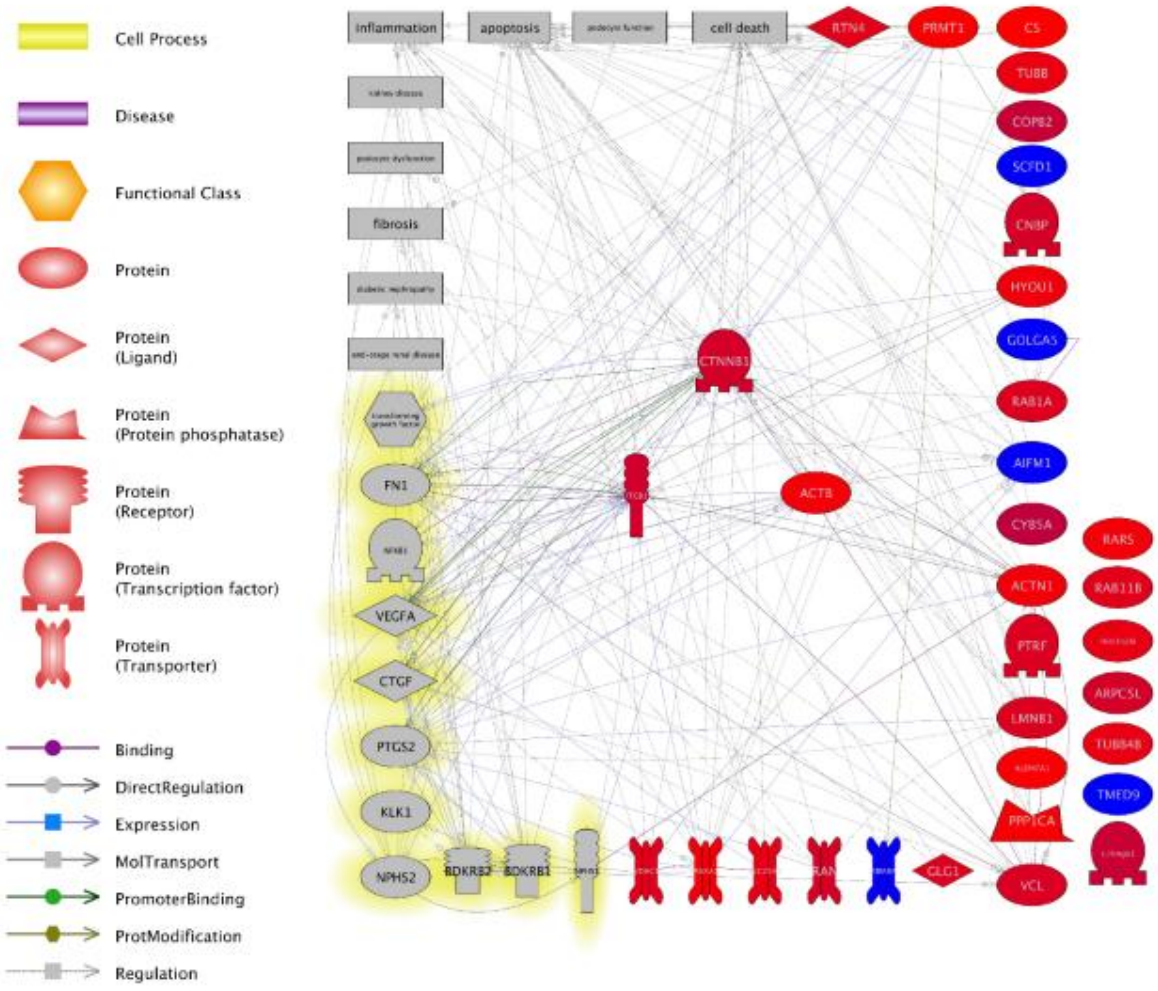
Cell Process
Disease
Functional Class
Protein
Protein (Ligand)
Protein (Protein phosphatase)
Protein (Receptor)
Protein (Transcription factor)
Protein (Transporter)
Binding
DirectRegulation
Expression
MolTransport
PromoterBinding
ProtModification
Regulation
inflammation
apoptosis
cell death
fibrosis
FN1
VEGFA
CTGF
PTGS2
KLK1
NPHS2
BDKRB2
BDKRB1
CTNNB1
ACTB
RTN4
PRMT1
CS
TUBB
COPB2
SCFD1
CNBP
HYOU1
GOLGA5
RAB1A
AIFM1
CYB5A
ACTN1
PTRF
LMNB1
TMED9
PPP1CA
VCL
CLG1
RARS
RAB11B
ARPC5L
TUBB4B

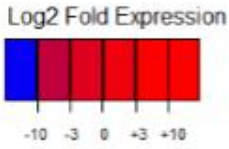
Log2 Fold Expression
-10
-3
0
+3
+10

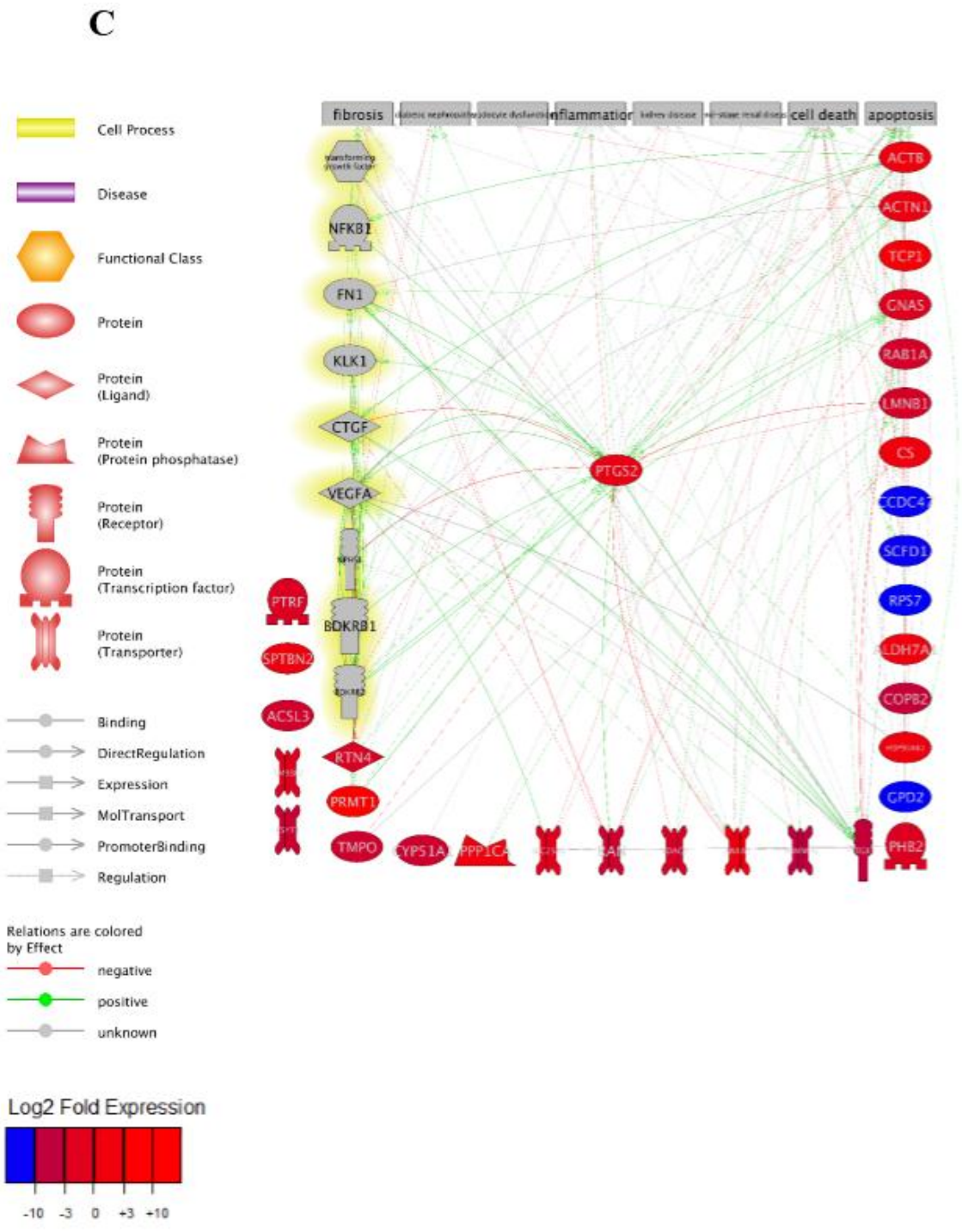

Figure 11: Pathway Studio Pathway Analysis linking the modified proteins in the different experiments to other proteins, cell processes, and diseases, with the highlighted components being manually introduced into the software. A: Modified proteins in the experiment comparing BK-treated podocytes for 3 hours to controls. B: Modified proteins in the experiment comparing BK-treated podocytes for 6 hours to controls. C: Modified proteins in the experiment comparing BK-treated podocytes for 3 hours to BK-treated podocytes for 6 hours.

Furthermore, due to the importance of COX-2 in our study, we construct a pathway tying it to the proteins that have been linked to it from all 3 experiments, along with the inputted suggested proteins and the cell processes and diseases. COX-2 possesses extended links to proteins related with diabetic nephropathy according to the literature, such as fibronectin, Kallikrein, VEGF-A, Connective Tissue Growth Factor (CTGF), Nephrin, and the Bradykinin receptors.

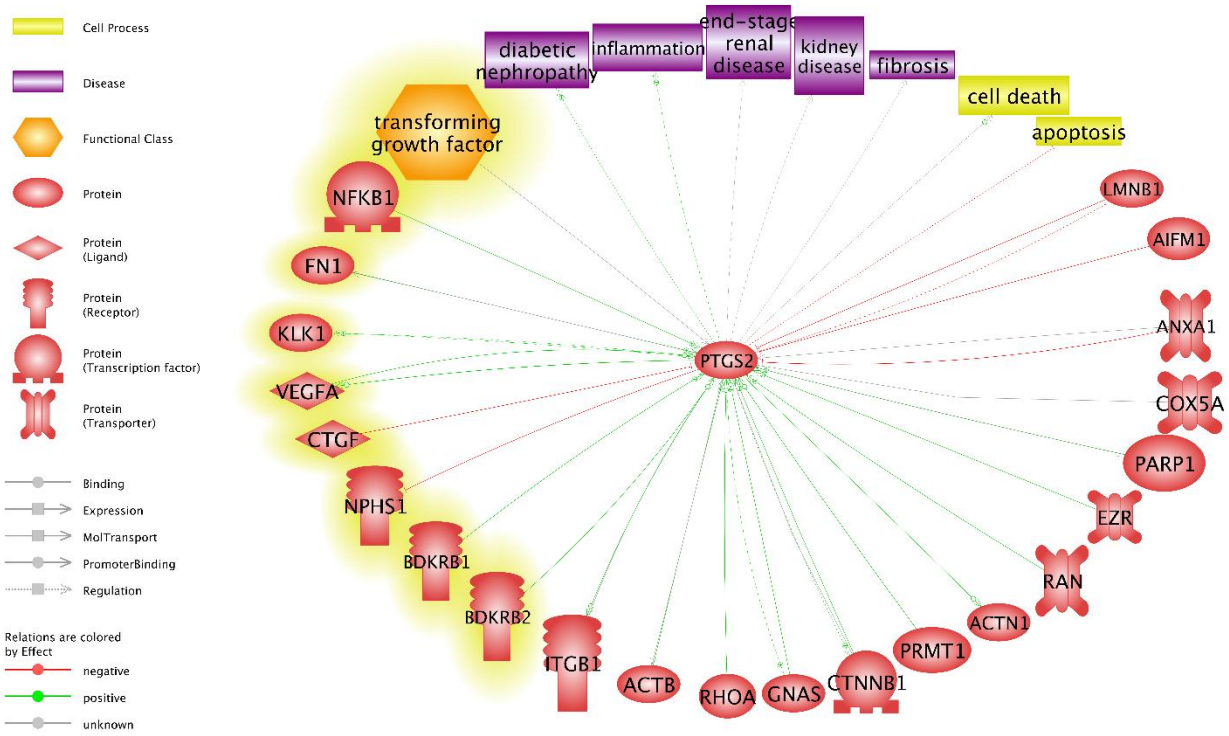

Figure 12: Pathway Studio analysis of the relationship for PTGS-2/COX-2 to different proteins, cell processes, and diseases, with the highlighted components being manually introduced into the software.

E. Enrichment Analysis of Expressed Proteins:

Using Ingenuity Pathway Analysis (IPA), we are able to translate the expressed transform our mass spectrometry data into suggested cellular processes and events with a colorimetric correlation value. This correlation value is based on:

- The number of proteins that support this event

- The expression levels of these proteins

- The expression of proteins that contradict this event

The software constructs a table of cellular phenomena ranked from highest to lowest correlation.

Below is IPA's "Diseases and Biological Functions" function based on our mass spectrometry data. The absence of a correlation, such as in the case of the first experiment "Control vs 3 hours BK treatment", corresponds to a lack of sufficient evidence for the software to claim an inhibition or promotion of the specific cellular event.

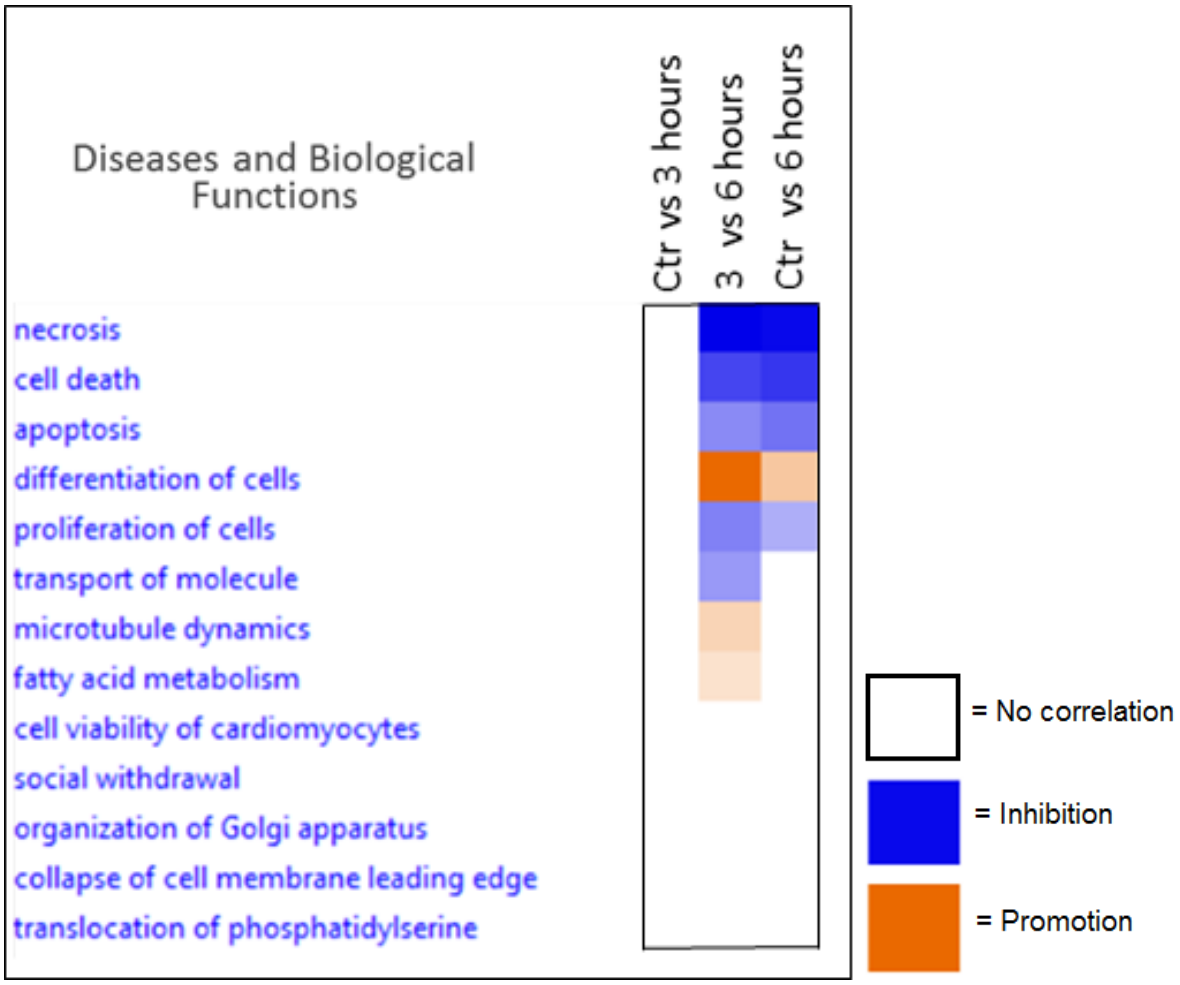

Figure 13: The diseases and biological functions suggested from IPA's analysis of the mass spectrometry results. The inhibition of Cell Death (as suggested by Necrosis, Cell Death, and Apoptosis) and the change in Cytoskeletal Activity (Unsure of the direction, as suggested by Transport of molecules and Microtubule Dynamics) were the most prominently suggested events.

As we can see in Figure 13, the most highly suspected diseases and biological functions, based on our protein data, fall under the umbrella of "inhibition of cell death" (inhibition of "necrosis", "cell death", and "apoptosis") and "change in cytoskeletal elements" (inhibition of "transport of molecules" and promotion of "microtubule

dynamics"). Furthermore, IPA allows us to construct individual figures for the different molecular and cellular phenomena, then display the linked proteins along with their links to the correlated phenomenon, whether positive or negative, and thus creating a suggested inhibition or promotion of that cellular phenomenon.

The following figures show the individual pathways from IPA's "Diseases and Biological Functions":

Cell Death: Ctr vs 6 hours Treatment

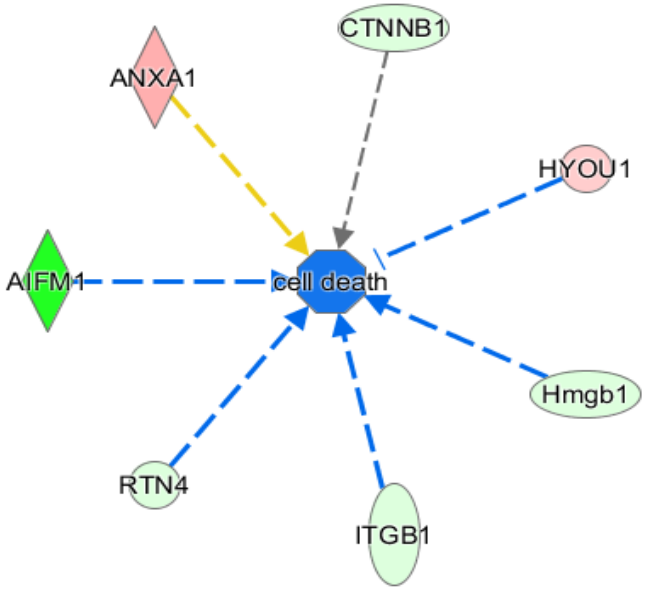

Apoptosis: Ctr vs 6 hours Treatment

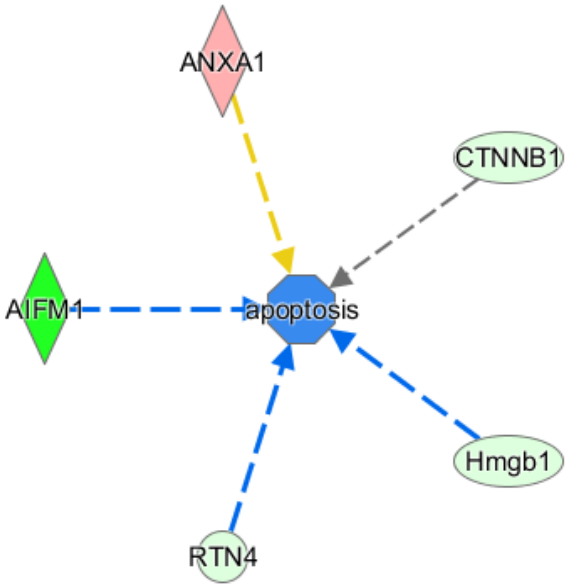

Necrosis: 3 vs 6 hours Treatment

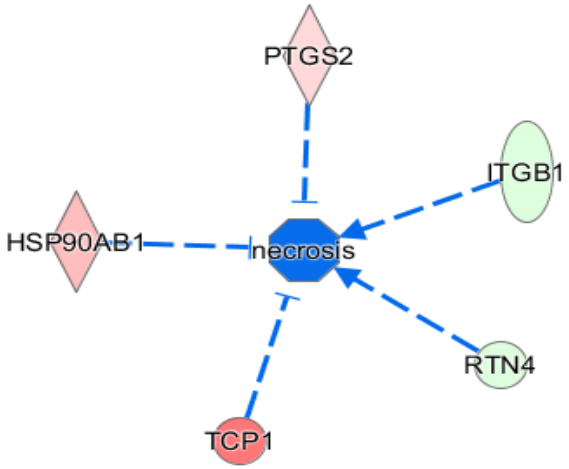

Cell Death: 3 vs 6 hours Treatment

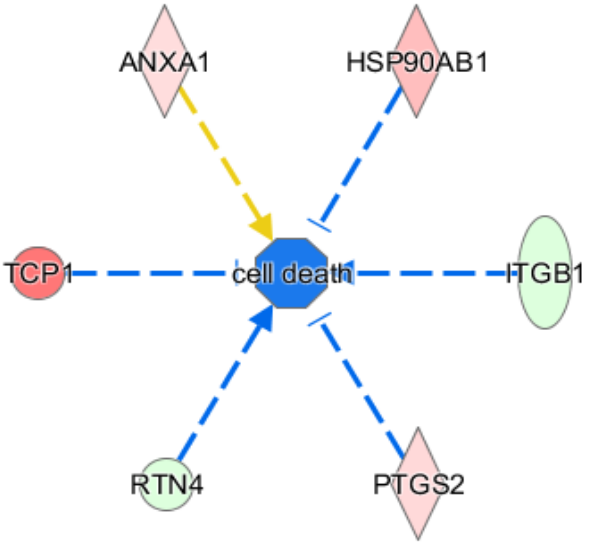

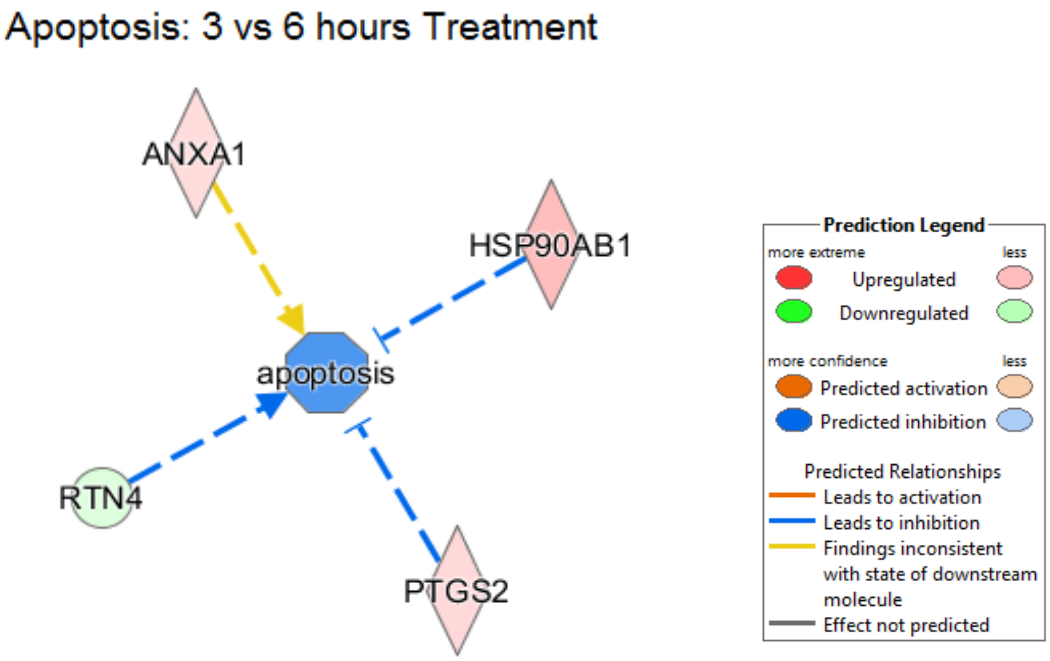

Figure 14: IPA's network analysis of different proteins from the different experiments, linking them to a suggested promotion or inhibition of a cellular event under the umbrella of inhibition of Cell Death, as previously suggested. A: Inhibition of Necrosis in the experiment comparing BK-treated podocytes for 6 hours versus controls. B: Inhibition of Cell Death in the experiment comparing BK-treated podocytes for 6 hours versus controls. C: Inhibition of Apoptosis in the experiment comparing BK-treated podocytes for 6 hours versus controls. D: Inhibition of Necrosis in the experiment comparing BK-treated podocytes for 3 hours versus BK-treated podocytes for 6 hours. E: Inhibition of Cell Death in the experiment comparing BK-treated podocytes for 3 hours versus BK-treated podocytes for 6 hours. F: Inhibition of Apoptosis in the experiment comparing BK-treated podocytes for 3 hours versus BK-treated podocytes for 6 hours.

Transport: Ctr vs 6 hours Treatment

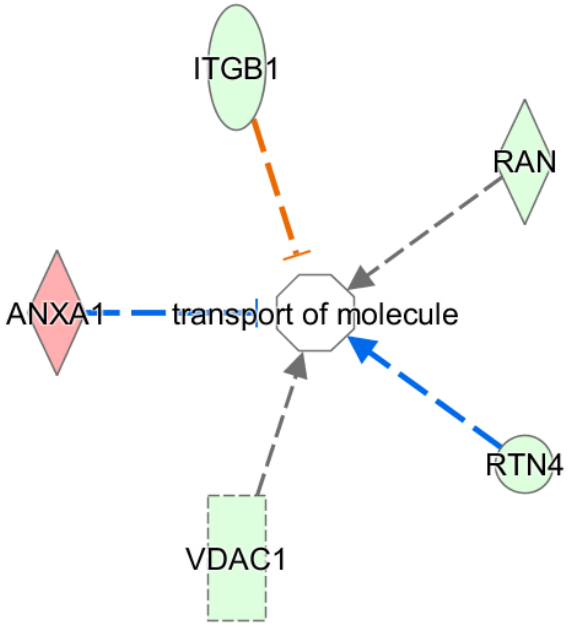

MT Dynamics: Ctr vs 3 hours Treatment

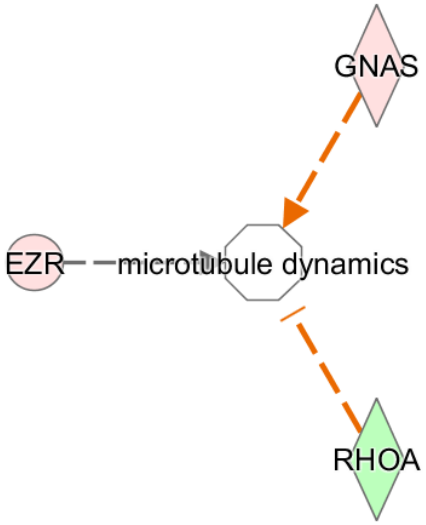

MT Dynamics: Ctr vs 6 hours Treatment

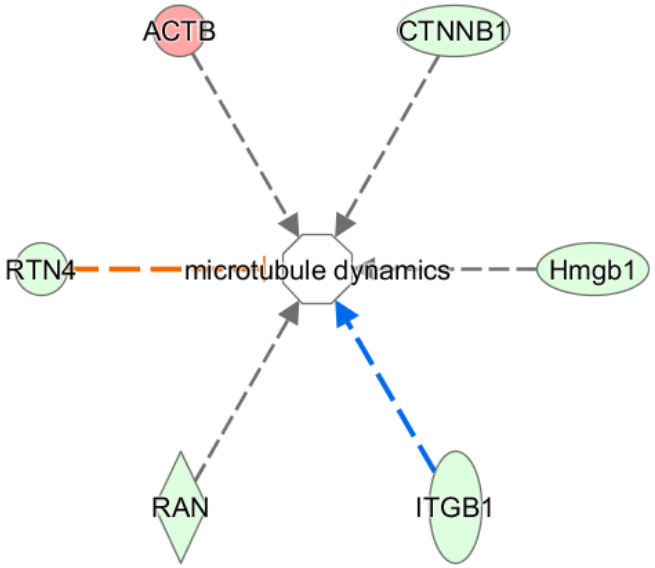

Transport: 3 vs 6 hours Treatment

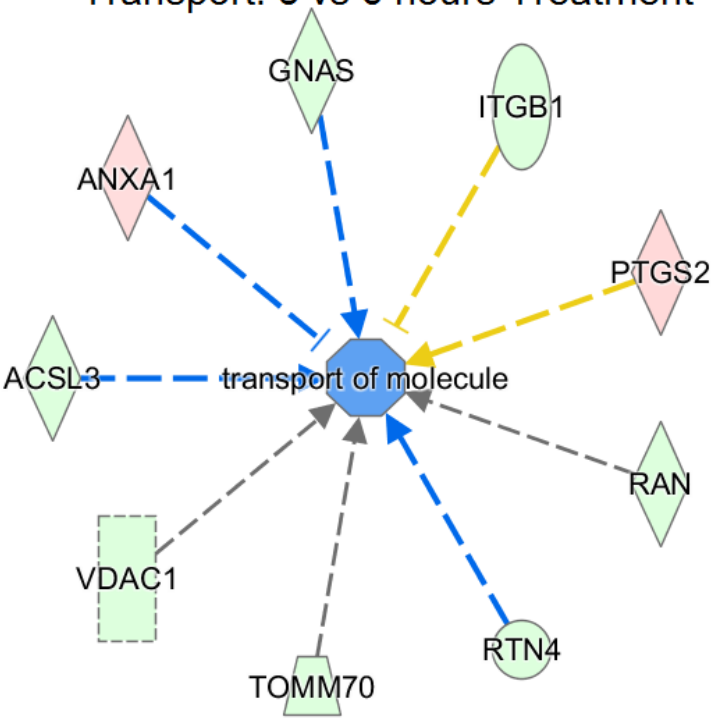

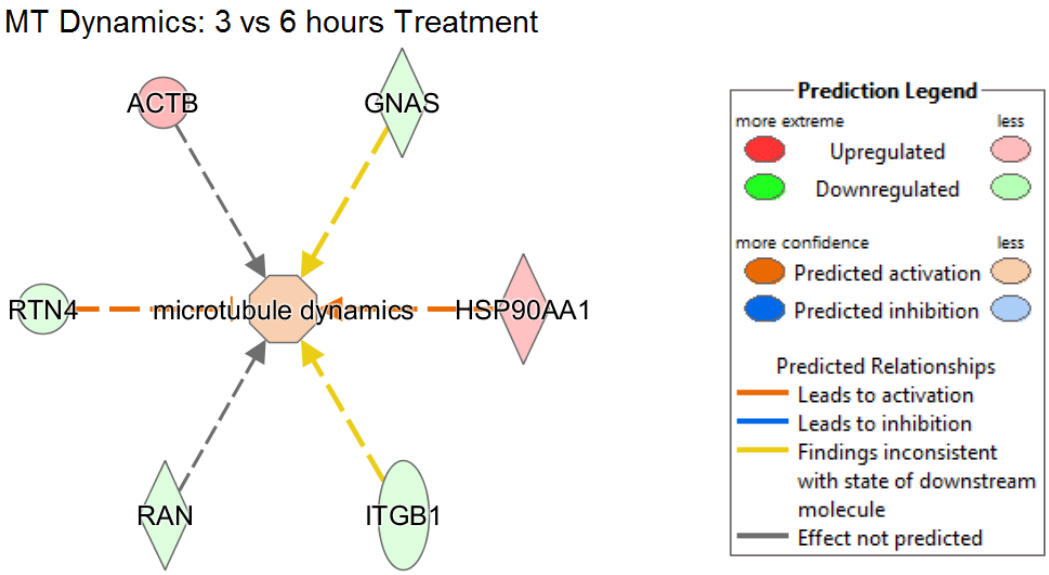

Figure 15: IPA's network analysis of different proteins from the different experiments, linking them to a suggested promotion or inhibition of a cellular event under the umbrella of Cytoskeletal Activity, as previously suggested. A: Suggestion of Microtubule Dynamics activity in the experiment comparing BK-treated podocytes for 3 hours vs control. B: Suggestion of Transport of Molecules activity in the experiment comparing BK-treated podocytes for 6 hours versus control. C: Suggestion of Microtubule Dynamics activity in the experiment comparing BK-treated podocytes for 6 hours versus control. D: Inhibition of Transport of Molecules in the experiment comparing BK-treated podocytes for 3 hours versus BK-treated podocytes for 6 hours. E: Activation of Microtubule Dynamics activity in the experiment comparing BK-treated podocytes for 3 hours versus BK-treated podocytes for 6 hours.

Other than providing insight into specific cellular mechanisms for every experiment on its own, IPA also allows us to view an aggregate of cellular mechanisms, grouped together by virtue of having common proteins between these processes, and present the protein expression in a network.

ID	Analysis	Molecules in Network	Top Diseases and Functions
1	3vs6 hours Log2	↑**ACTB,** ↑**ACTN1,** ↑**ALDH7A1,** ALOX5, AP3D1, BRDT, CHMP2B, ↑**CS,** F2R, GDI1, ↓**GNAS,** ↑**HSP90AA1,** ↑**HSP90AB1,** IL1R1, ↓**ITGB1,** KATNA1, KCNJ11, Ldha/RGD1562690, MYC, NFkB (complex), ↓**PHB2,** ↑**PPP1CA,** ↑**PRMT1,** PTGER2, PTGER4, ↑**PTGS2,** PXN, ↓**RAN,** ↑**SPTBN2,** STUB1, ↑**TCP1,** TNF, TSPO, ↓**VDAC1,** VIM	Cell Death and Survival, Cancer, Gastrointestinal Disease
1	0vs6 hours Log2	↑**ACTB,** ↓**AIFM1,** Akt, ↑**ANXA1,** CAST, CCND1, CDH2, CDKN1A, ↓**CNBP,** CPE, CRYAB, ↑**CS,** ↓**CTNNB1,** GSK3B, ↓**Hmgb1,** HSPE1, IGF1R, ↓**ITGB1,** KCNJ11, MMP9, MYC, MYO1C, OTOF, ↑**PRMT1,** PTK2, PXN, ↑**RARS,** SLC12A2, TNF, TP53, TSC2, TSPO, ↓**TUBB,** ↓**VDAC1,** VIM	Cell Death and Survival, Skeletal and Muscular Disorders, Cellular Movement
1	0vs3 hours Log2	↓**ACLY,** AGTR2, calpain, CASP3, CCL5, DLAT, ERK1/2, FOS, GAPDH, ↑**GNAS,** HADHA, IGF1, IL6, IL1B, Jnk, KCNJ11, MAPK1, NFkB (complex), NMDA Receptor, P38 MAPK, ↑**PARP1,** PC, PCSK6, ↓**PDHB,** PPARG, PRKCD, PRKD1, PTK2B, RAC1, ↓**RACK1,** ↓**RHOA,** SLC1A2, ↑**SLC25A3,** SP1, TNF	Cell Death and Survival, Skeletal and Muscular Disorders, Cancer
2	0vs6 hours Log2	↑**ACTN1,** CHMP2B, ↑**PPP1CA,** ↓**RAN,** ↓**VCL**	Hereditary Disorder, Neurological Disease, Organismal Injury and Abnormalities
2	0vs3 hours Log2	DCC, ↑**EZR,** Podxl, PSMA1	Cancer, Organismal Injury and Abnormalities, Cell Morphology
2	3vs6 hours Log2	GRM4, ↓**RAB1A**	Cell Morphology, Cellular Assembly and Organization, Inflammatory Disease
3	0vs6 hours Log2	↑**ALDH7A1,** NFkB (complex)	Hereditary Disorder, Neurological Disease, Organismal Injury and Abnormalities
3	3vs6 hours Log2	BET1L, ↓**COPB2**	Infectious Diseases, Cell Death and Survival, Cellular Assembly and Organization
4	0vs6 hours Log2	GRM4, ↓**RAB1A**	Cell Morphology, Cellular Assembly and Organization, Inflammatory Disease
4	3vs6 hours Log2	SET, ↓**SLC25A5**	Cellular Compromise, Cellular Development, Cellular Growth and Proliferation
5	3vs6 hours Log2	↑**ANXA1,** PRL, TSC2	Cell Morphology, Organ Morphology, Endocrine System Development and Function

Figure 16: Network analysis of IPA showing the top diseases and functions linked to the proteins identified by the mass spectrometry in their individual experiments.

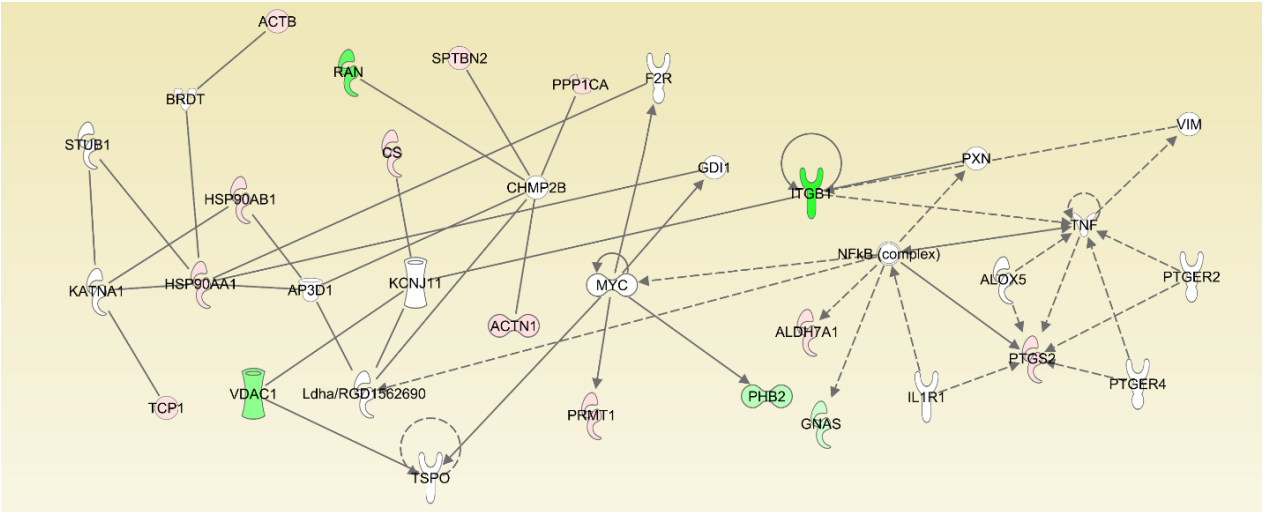

Figure 17: The network titled “Cell Death and Survival, Cancer, GI Disease” of the 3vs6 hours experiment in the network analysis function of IPA

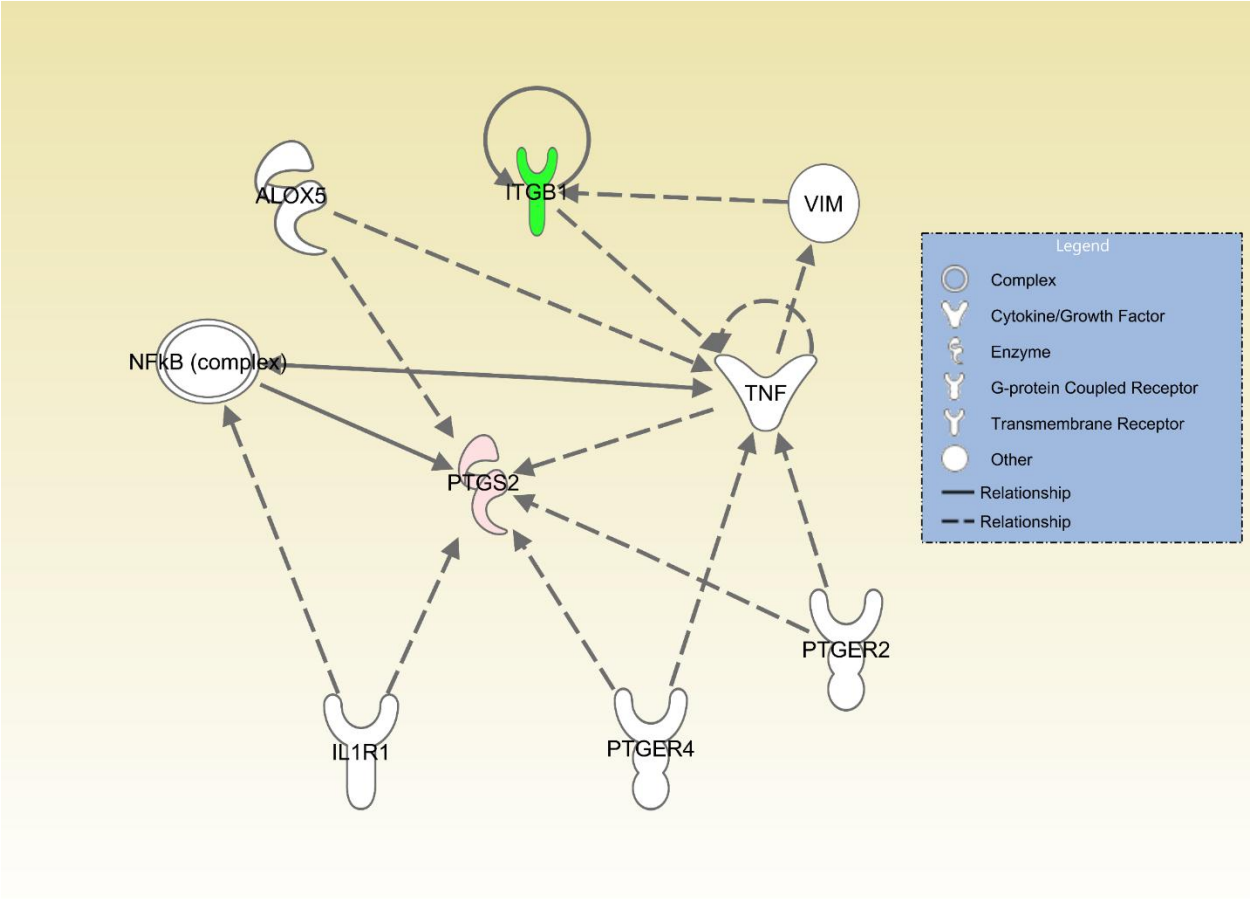

Figure 18: A subset of the previous network titled “Cell Death and Survival, Cancer, GI Disease” with a focus on PTGS-2’s place in the network and its neighbouring molecules.

F. Validation of the Proteomic Data

1. COX-2 is upregulated by BK Treatment

In order to confirm the results of the mass spectrometry procedure, we set out to validate COX-2's increase in protein level resulting from BK treatment.

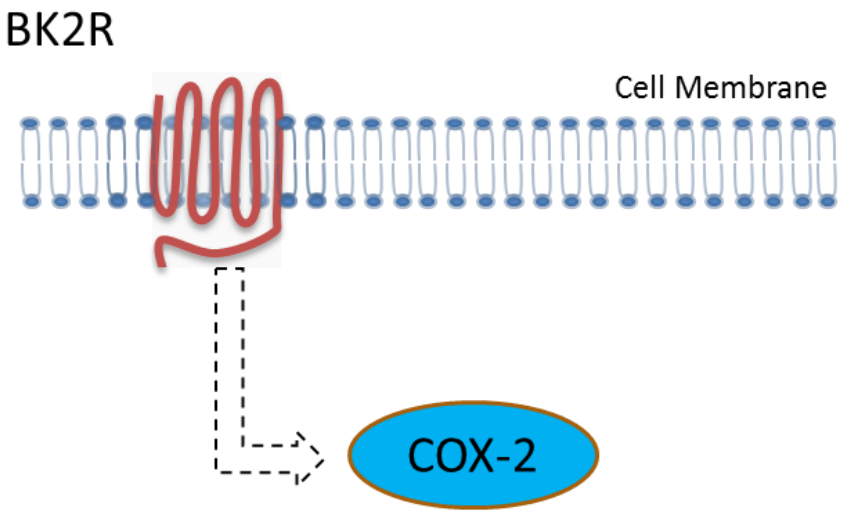

Figure 19: Schematic representing the question we aim to address in this experiment, where we want to validate if the activation of the Bradykinin-2-Receptor (BK2R) by the action of BK treatment leads to the upregulation of the COX-2 protein level.

Plated quiescent podocytes were treated with BK at 10^{-7} M for different timepoints, Phorbol-12-myristate-13-acetate (in a DMSO vehicle) was used on the cells as a positive control for COX-2 expression (PMA greatly stimulated COX-2), then the cells were lysed and the proteins were immunoblotted. COX-2 protein levels have indeed increased upon BK treatment.

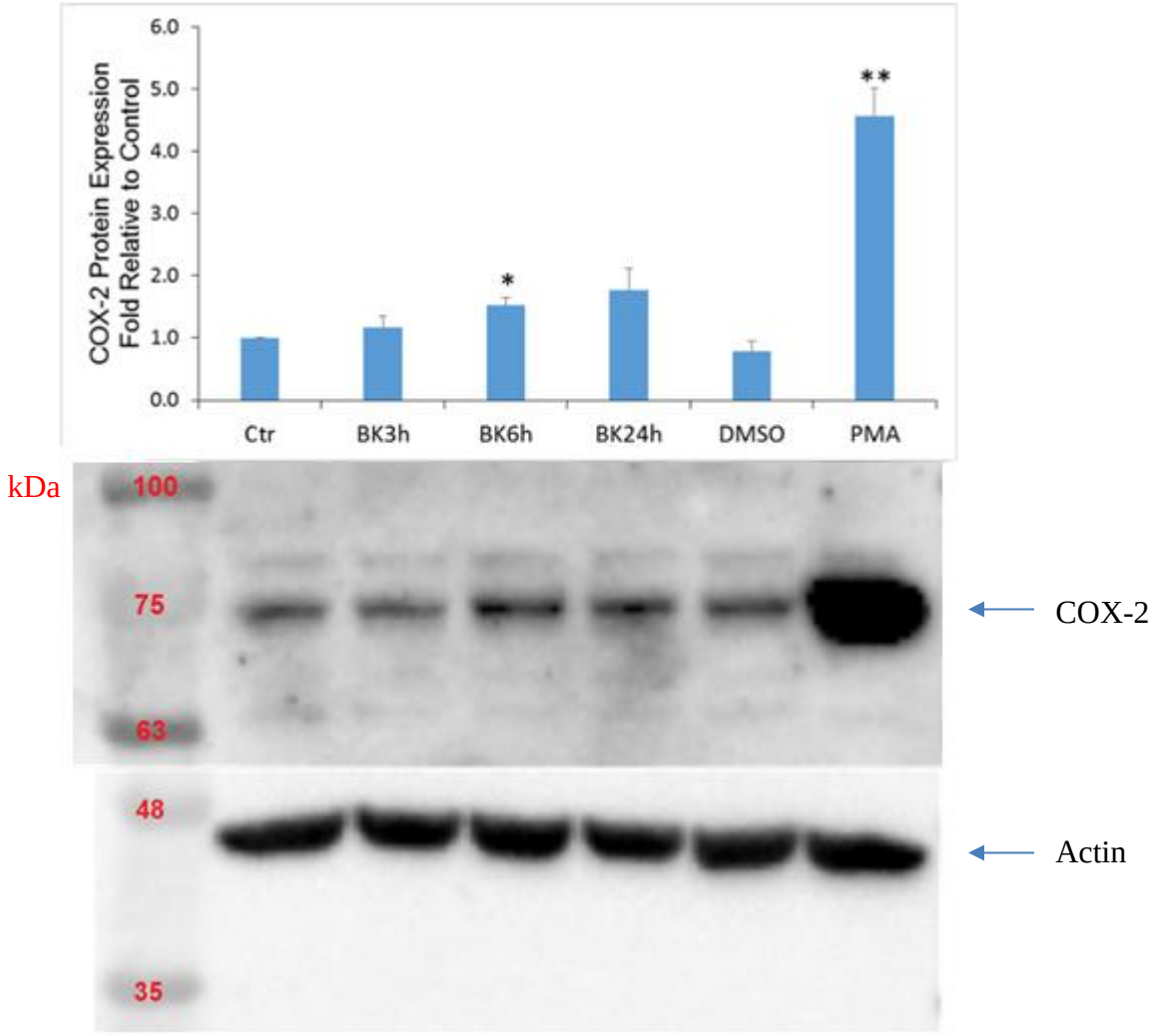

Figure 20: BK stimulated COX-2 protein expression in podocytes. Quiescent podocytes were stimulated with BK (10^{-7} M) for 3, 6, and 24 hours, as well as stimulated with the known COX-2 activator Phorbol-12-myristate-13-acetate (PMA) (10^{-6} M) and its vehicle Dimethyl Sulfoxide (DMSO) (10^{-6} M). COX-2 and Actin levels were measured by western blot. Bar graph represents the fold change in protein levels of COX-2 (*p=0.012 BK 6h vs Control, **p=0.0013 PMA 6h vs DMSO) relative to Actin protein levels and is the sum of more than 3 separate experiments.

BK treatment leads to an increase in COX-2 protein level. However, the next question is: does this increase in protein level correlate with an increase in COX-2 activity levels? The next experiment measures the level of the COX-2-downstream metabolite PGE_2 in the supernatant in the media, which can be a marker of COX activity.

2. *BK Treatment leads to the increase in PGE_2 production:*

COX activity leads to PGE_2 release in the supernatant. We measure BK's increase of PGE_2 production in the supernatant by the enzyme immunoassay (EIA) experiment.

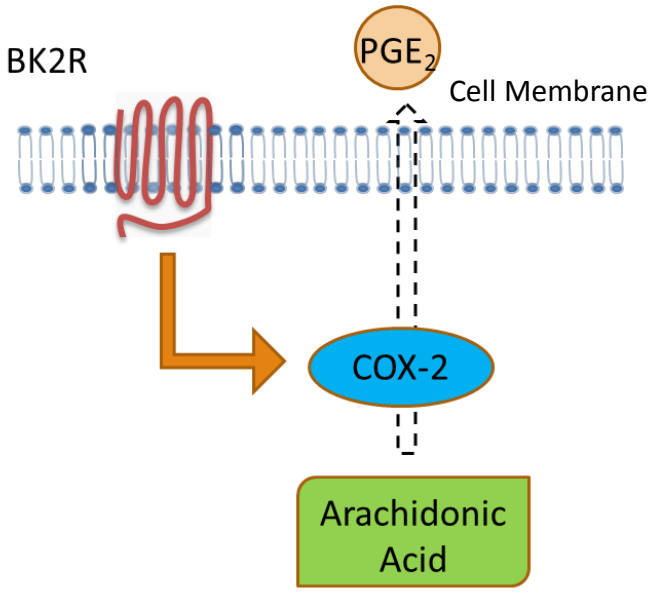

Figure 21: Schematic representing the question we aim to address in this experiment, where we want to check if the activation of the BK2R by BK leads to an increase in COX-2-downstream metabolite PGE_2 levels in the supernatant.

In this first EIA experiment, media of plated podocytes treated with BK at 10^{-7} M was collected and PGE_2 levels were measured at 3, 6, and 24 hours following BK treatment. We can see that the longer treatment with BK is associated with an increased PGE_2 level in the supernatant. That is to be expected due to a suspected longer time of COX-2 activity, and bearing in mind that podocytes have basal COX-2 activity.

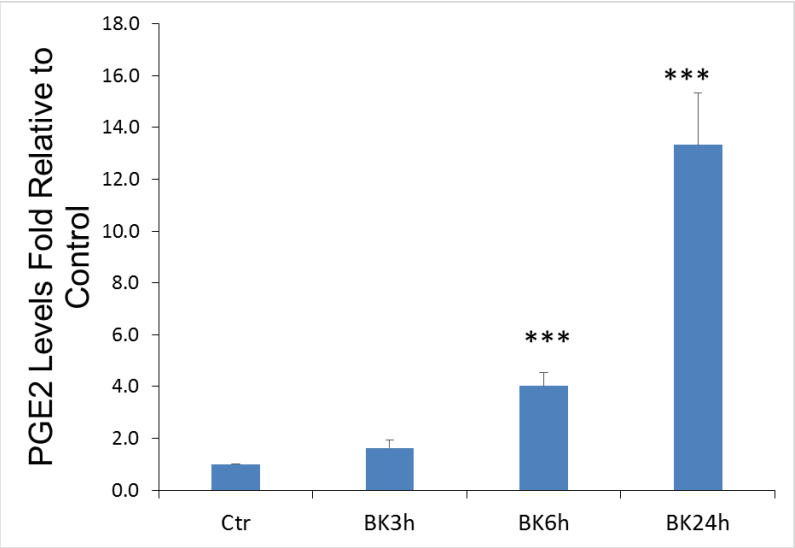

Figure 22: BK stimulated PGE_2 release in podocytes. Quiescent podocytes were stimulated with BK (10^{-7} M) for 3, 6, and 24 hours. PGE_2 levels were measured by Enzyme Immunoassay (EIA) with a sensitivity of 0.35 pg/mL. Bar graph represents the fold change in measured PGE_2 levels (***$p<0.001$ BK 6h vs Control, ***$p<0.001$ BK 24h vs Control) and is the sum of more than 3 separate experiments.

3. Ibuprofen inhibits the BK induction of PGE_2 production

We saw the increase of PGE_2 levels due to BK treatment. Now, we want to see if the introduction of the NSAID and COX inhibitor Ibuprofen stops the PGE_2 levels increase due to BK.

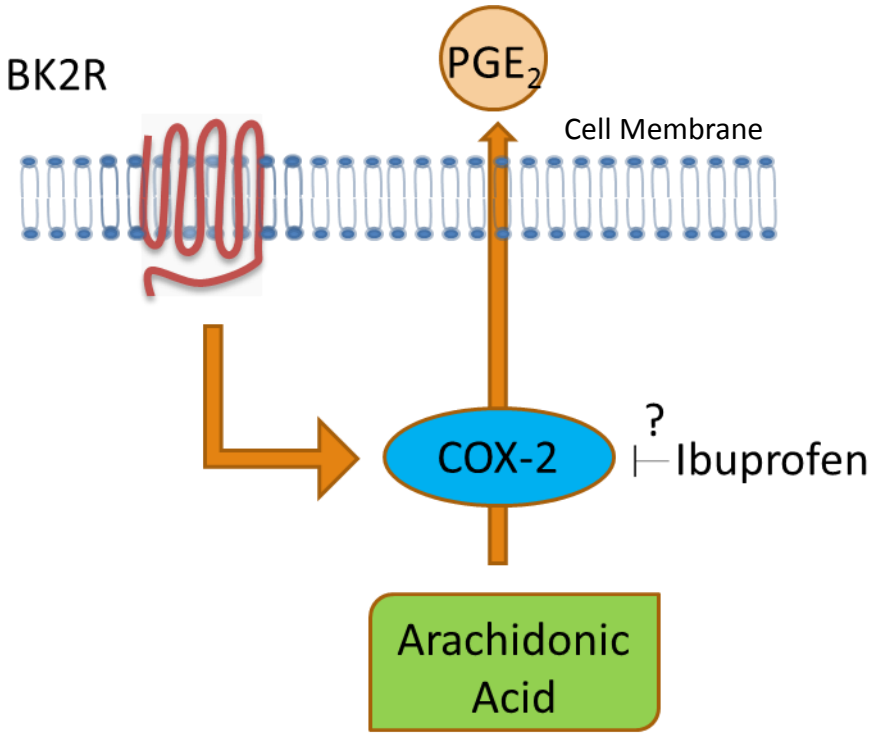

Figure 23: Schematic representing the question we aim to address in this experiment, where we want to check if the introduction of the NSAID and COX inhibitor Ibuprofen leads to the inhibition of the PGE_2 level increase associated with BK treatment.

Media of quiescent podocytes treated with BK at 10^{-7} M and with a subset of them treated with Ibuprofen at 10^{-6} M was collected at 6 hours in addition to control podocytes, and PGE_2 levels were measured by the EIA experiment. We can see that BK's stimulation of PGE_2 production is inhibited by Ibuprofen at 6 hours.

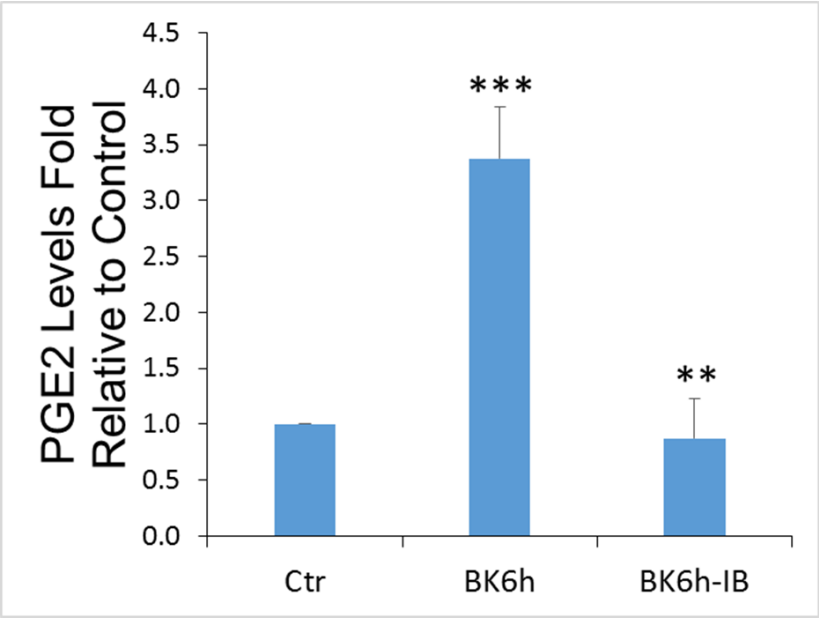

Figure 24: BK stimulated PGE_2 release in podocytes, and Ibuprofen downplayed this release. Quiescent podocytes were stimulated with BK (10^{-7} M) for 6 hours and a portion of them with Ibuprofen (10^{-6} M) one hour prior to BK stimulation. PGE_2 levels were measured by Enzyme Immunoassay (EIA) with a sensitivity of 0.35 pg/mL. Bar graph represents the fold change in measured PGE_2 levels (***$p<0.001$ BK 6h vs Control, **$p=0.0025$ BK 6h-IB vs BK 6h) and is the sum of at least 3 separate experiments.

4. BK Treatment leads to an increase in ERK phosphorylation:

From the literature, it has been suggested that one of the downstream pathways of BK treatment leads to the phosphorylation of the p42/44 ERK protein levels. So we run a western blot to confirm if the BK stimulation leads to phosphorylation of the ERK protein.

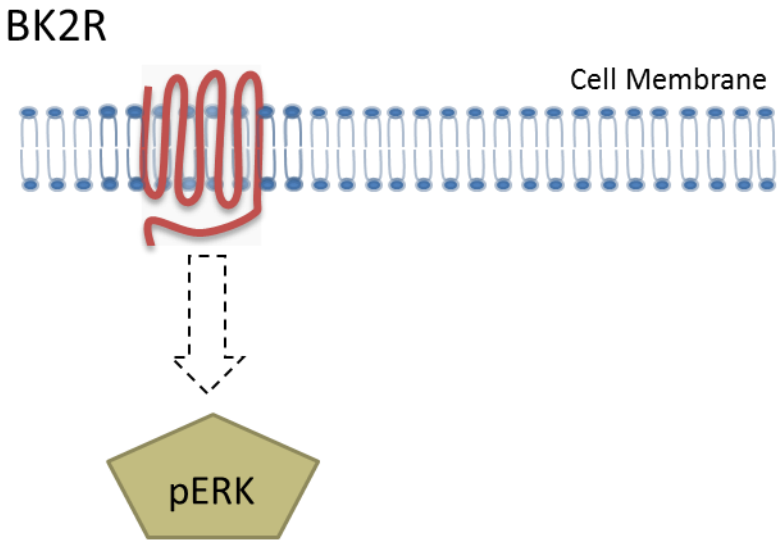

Figure 25: Schematic representing the question we aim to address in this experiment, where we want to check if the BK treatment leads to the phosphorylation of the p42/44 ERK protein.

Plated quiescent podocytes treated with BK at 10^{-7} M for 5, 10, and 30 minutes in addition to 3 and 6 hours were lysed and immunoblot experiments took place. We can see that BK's stimulation has increased the phosphorylated ERK protein levels starting at 5 minutes.

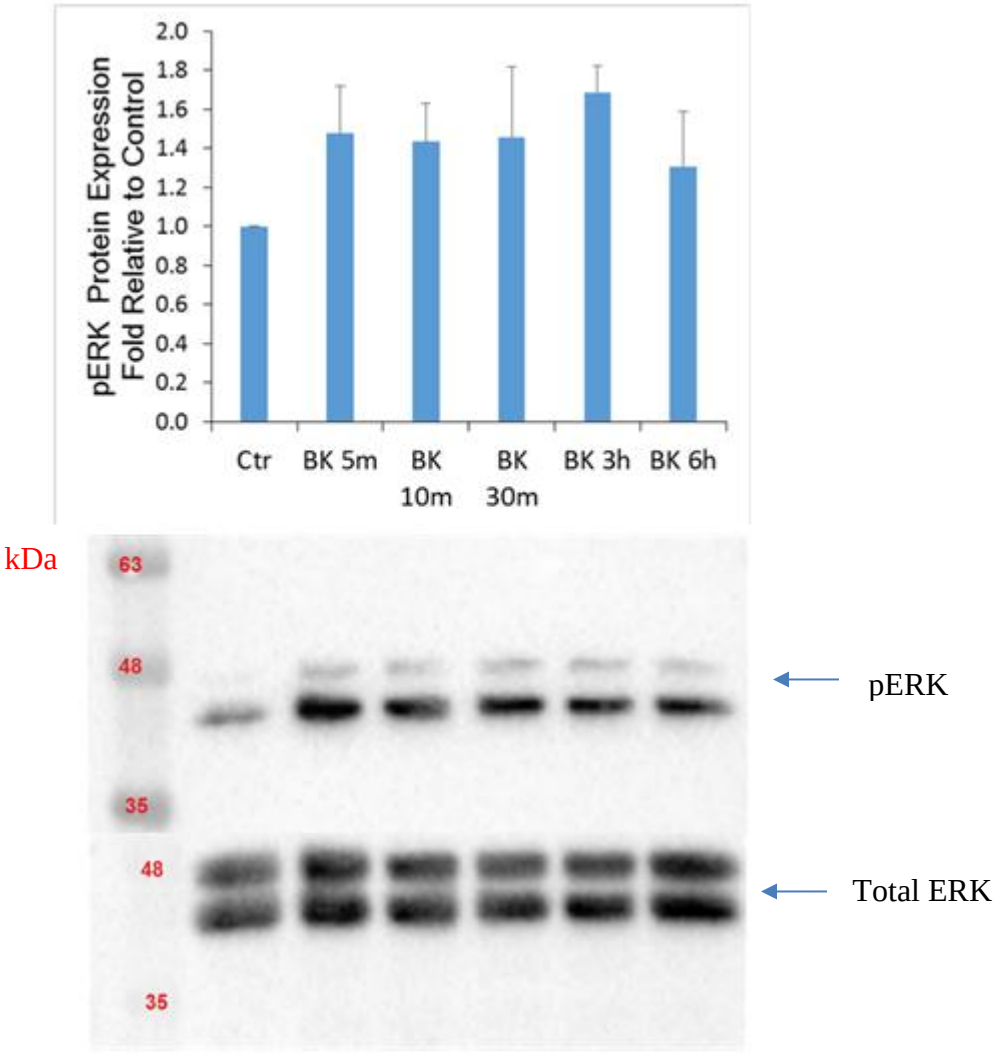

Figure 26: BK stimulated pERK protein expression in podocytes. Quiescent podocytes were stimulated with BK (10^{-7} M) for 5, 10, 30 minutes and 3 and 6 hours. pERK and total ERK (as a loading control) levels were measured by western blot. Bar graph represents the fold change in protein levels of pERK relative to total ERK protein levels and is the sum of 3 separate experiments.

5. PD98059 inhibits the BK induction of PGE_2 production:

We saw that one of the downstream pathways affected by BK treatment is the phosphorylation of ERK. However, is that same pathway also responsible for the increase

in PGE_2 levels in the supernatant? To that end, we use the MEK inhibitor (upstream of ERK) PD98059 and observe the PGE_2 levels between the experimental groups.

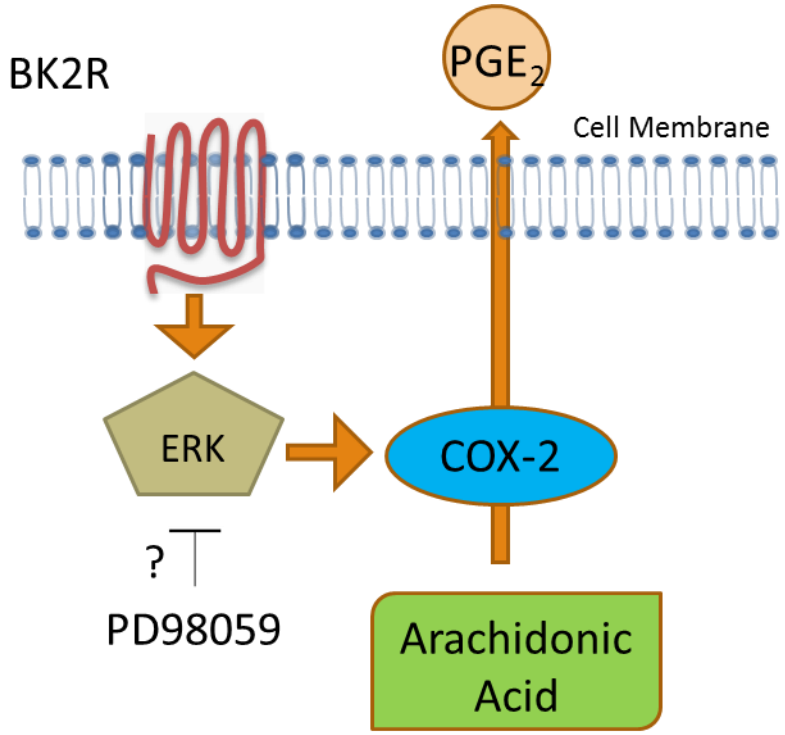

Figure 27: Schematic representing the question we aim to address in this experiment, whether the stimulation of PGE_2 in response to BK treatment is inhibited by the introduction of the MEK (upstream of ERK) inhibitor PD98059.

Media from plated quiescent podocytes treated with BK at 10^{-7} M and a subset of them additionally treated with PD98059 at 25 μM was collected and PGE_2 levels were measured by the EIA experiment. We can see that BK's stimulation of PGE_2 was inhibited by PD98059 at 6 hours.

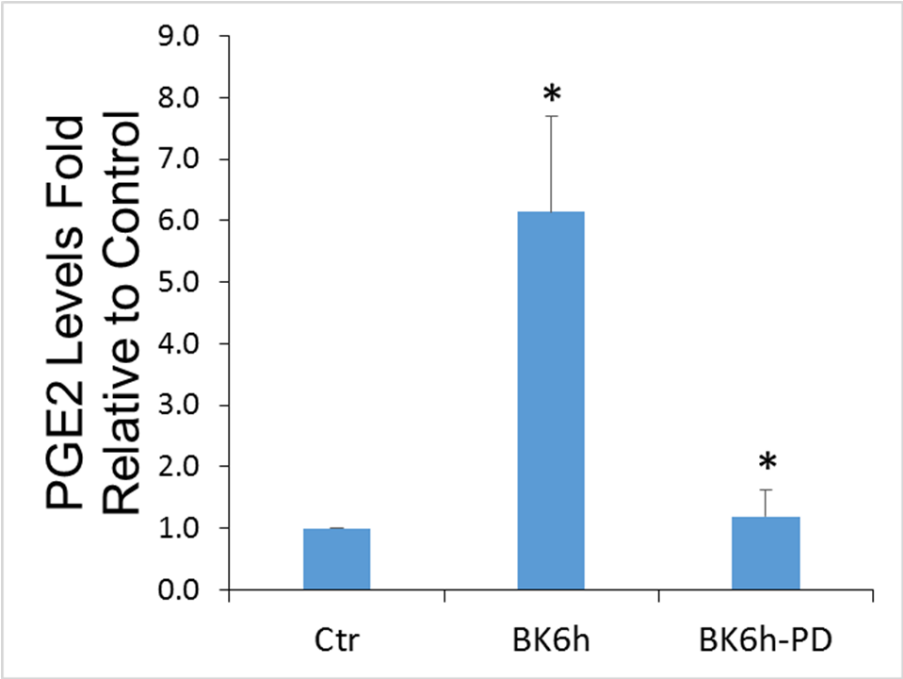

Figure 28: BK stimulated PGE_2 release in podocytes, and PD98059 downplayed this release. Quiescent podocytes were stimulated with BK (10^{-7} M) for 6 hours and a portion of them with PD98059 (25 μM) one hour prior to BK stimulation. PGE_2 levels were measured by Enzyme Immunoassay (EIA) with a sensitivity of 0.35 pg/mL. Bar graph represents the fold change in measured PGE_2 levels (*p<0.0292 BK 6h vs Control, *p=0.0366 BK 6h-PD vs BK 6h) and is the sum of at least 3 separate experiments.

6. Ibuprofen and PD98059 demonstrate their effect early on:

We saw that Ibuprofen and PD98059 both downplay BK's increase in PGE_2 production at 6 hours. However, does the PGE_2 production start early on? And do the inhibitors mediate their effect at that time?

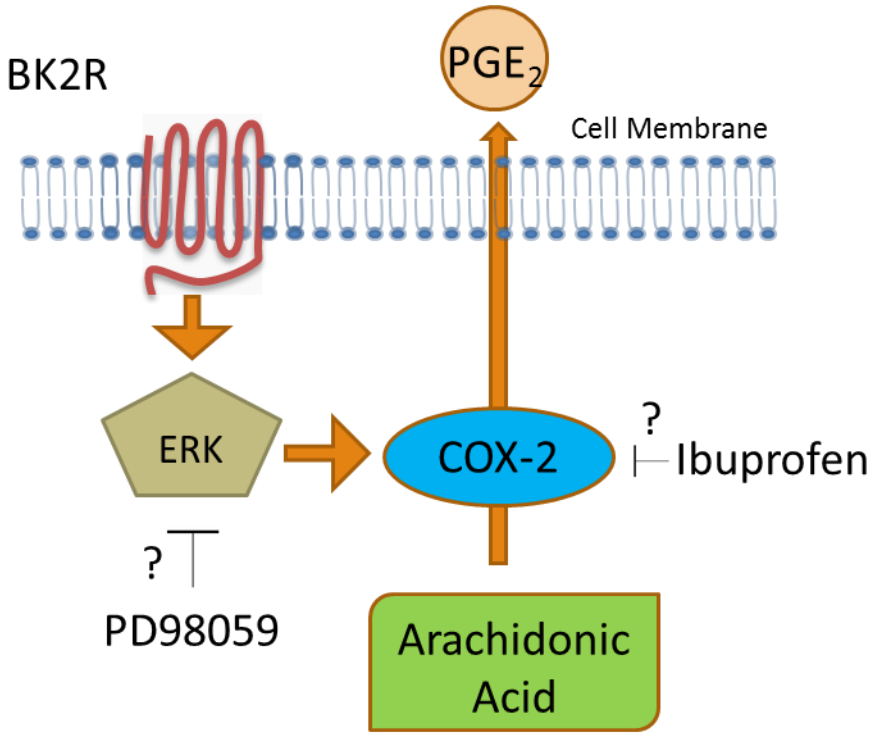

Figure 29: Schematic representing the question we aim to address in this experiment, whether the production of PGE_2 begin as early as 5 minutes, and whether the inhibitors mediate their effect that early on.

Media of plated quiescent podocytes treated with BK at 10^{-7} M, Ibuprofen at 10^{-6} M, and PD98059 at 25 μM was collected and PGE_2 levels were measured by the EIA experiment. We can see that BK's stimulation of PGE_2 production and inhibition by Ibuprofen and PD98059 start as early as 5 minutes.

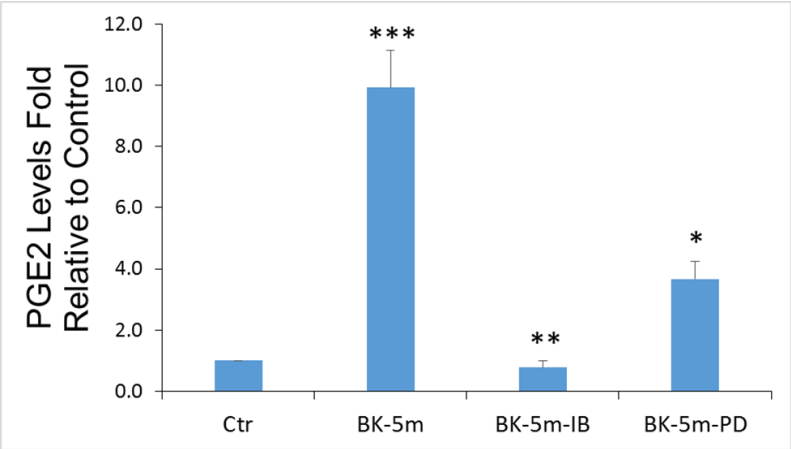

Figure 30: BK stimulated PGE_2 release in podocytes at short time, and Ibuprofen and PD-98059 downplayed this release. Quiescent podocytes were stimulated with BK (10^{-7} M) for 3, 6, and 24 hours and a portion of them with PD98059 (25 μM) one hour prior to BK stimulation, and another portion of them with Ibuprofen (10^{-6} M) one hour prior to BK stimulation. PGE_2 levels were measured by Enzyme Immunoassay (EIA) with a sensitivity of 0.35 pg/mL. Bar graph represents the fold change in measured PGE_2 levels (***p<0.001 BK 5m vs Control, **p=0.0014 BK 5m-IB vs BK 5m, *p=0.0115 BK 5m-PD vs BK 5m) and is the sum of at least 3 separate experiments.

7. Nephrin is downregulated by BK treatment:

Nephrin is an important marker for podocyte function, as mentioned previously.

We want to see if BK treatment leads to a change in podocyte protein expression.

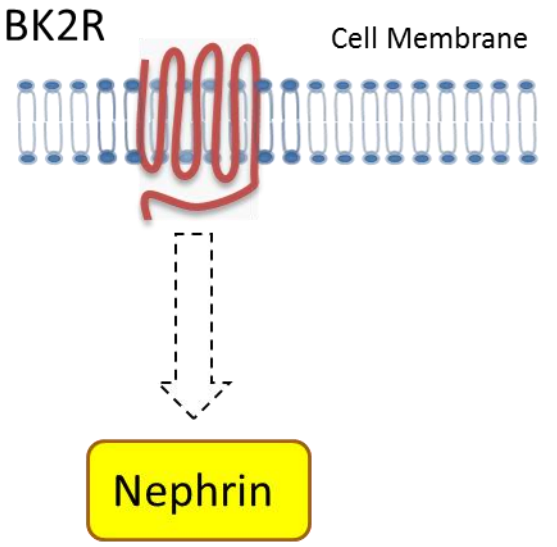

Figure 31: Schematic representing the question we aim to address in this experiment, whether Nephrin protein levels are affected by BK treatment.

Plated quiescent podocytes were treated with BK at 10^{-7} M at 6 hours, then the cells were lysed and immunoblot experiments occurred. We can see that BK stimulation leads to a decrease in Nephrin protein level at 6 hours.

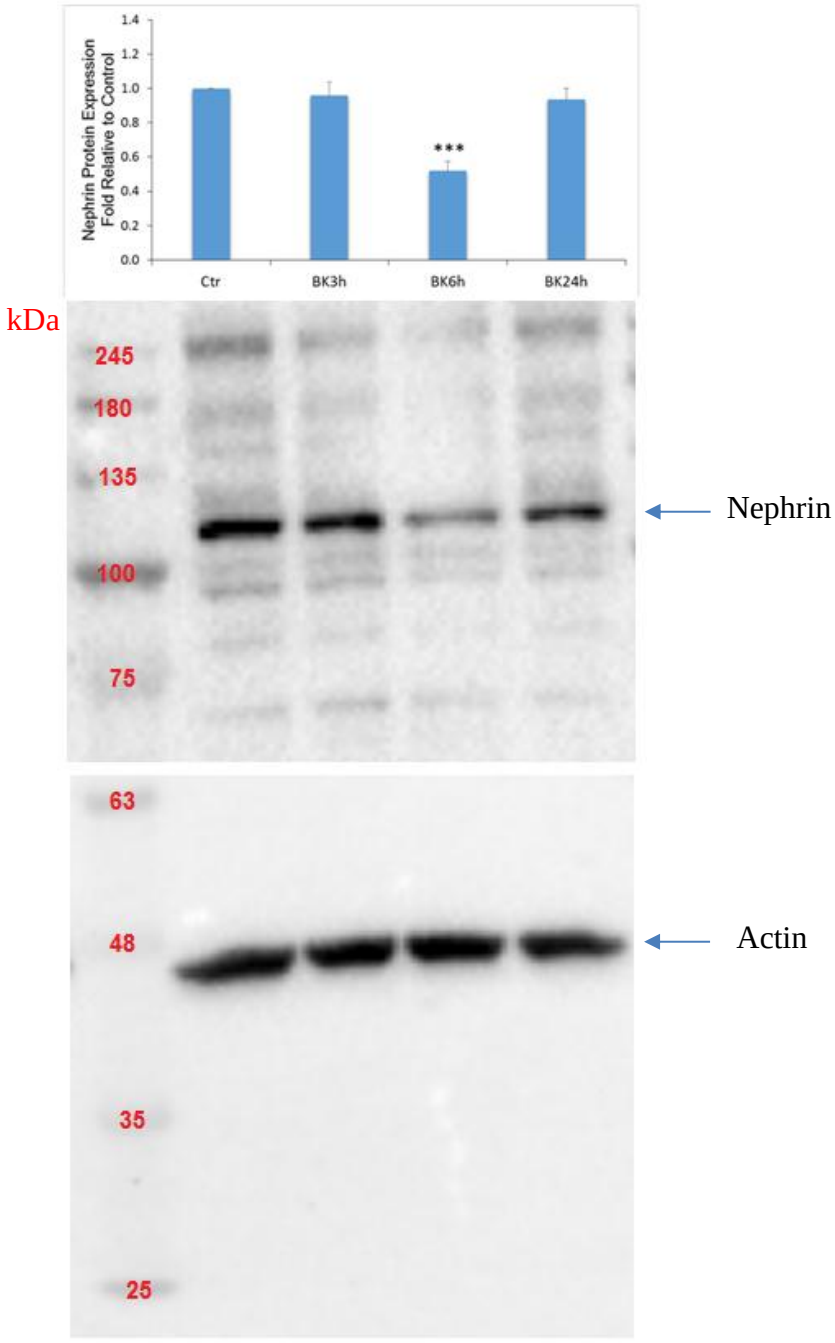

Figure 32: BK reduced Nephrin protein expression in podocytes. Quiescent podocytes were stimulated with BK (10^{-7} M) for 3, 6, and 24 hours. Nephrin and Actin levels were measured by western blot. Bar graph represents the fold change in protein levels of Nephrin relative to Actin protein levels (***$p<0.0001$ BK 6h vs Control) and is the sum of more than 3 separate experiments

CHAPTER IV

DISCUSSION:

The advent of proteomic analysis has revolutionized the way we understand the cellular processes of a specific population of cells, and by extension, the different cellular phenomena and pathologies these cells might be related to. Our global proteomic analysis of podocytes, other than being one of few studies to conduct LC-MS/MS analysis on podocyte cell-lysates, has shed light on the different cellular processes occurring, whether at control conditions or with BK treatment. Some of the proteins of particular interest, based on the suggested links to other proteins and relevant cellular processes as highlighted by our systems biology, that have showed up in the protein profile include: RHOA, β-Catenin, Integrin-β1, Apoptosis-Inducing Factor (AIFM-1), and PTGS-2 (COX-2). RhoA has generally been identified as a classic player in the cytoskeletal rearrangement pathway [91], which is of importance to us considering that podocyte cell death is usually accompanied by cytoskeletal rearrangements in the form of detachment from the glomerular basement membrane [92]. This result is consistent with another study showing a downregulation of RhoA in a podocyte injury model, and where the knock-down of RhoA by siRNA has shown increased podocyte apoptosis [93]. β-Catenin is another protein implicated in cytoskeletal rearrangement activities, as it interacts with the cytoplasmic regions of cadherin, serves the crucial role of regulating the adherens junctions, as well as participating as a key player in the Wnt signaling pathway [94]. Previous research also

indicated a decrease in β-catenin in a diabetic nephropathy model, where both the protein levels and the mRNA levels of β-catenin were decreased in hyperglycemic conditions with the presence of AGEs [94], consistent with the decrease observed in our proteomics data. Integrin-β1 has also been associated with podocyte health, where a study showed that mice with specific Integrin-β1 deletions cannot complete postnatal renal development, and die of proteinuria [95], suggesting a possible role of the downregulation of Integrin-β1 in the progression of diabetic nephropathy. AIFM-1 (Apoptosis-inducing factor 1) is a protein that is recruited to the nucleus when apoptotic signals are initiated, where it will lead to DNA fragmentation [96]. However, no studies have been conducted on the activation of AIFM-1 in podocytes, especially bearing in mind that podocytes are known to die by apoptosis in diabetic nephropathy conditions [92]. PTGS-2 (COX-2) has been implicated in several studies, where its inhibition in podocytes reduced proteinuria in a glomerular injury model [73], and where BK has been shown to induce COX-2 in glioma cells [97], human airway smooth muscle cells [98], renal thick ascending limb cells [99], and increased COX-2 mRNA in endotoxin-treated porcine coronary artery [100]. However, no study has yet demonstrated the upregulation of COX-2 due to BK treatment in podocytes, which we have shown in our proteomics data and validated in our western blots. Systems biology analysis has performed 2 functions in our research: it suggested physiological and pathological processes underlying the change in protein profile of the BK-treated podocytes, and it suggested the pathways linking our observed proteins with other suggested proteins based on the software knowledgebase. The main processes suggested to be occurring were those related to cell death (named by the software: “Apoptosis”, “Necrosis”, and “Cell Death”) and those related to cytoskeletal remodeling (named by the software: “Microtubule

Dynamics" and "Transport of Molecules"). The systems biology analysis seemed to point at an inhibition of cell death, even though the literature suggests that upregulation of COX-2 (by BK treatment) has been linked to podocyte loss [43,73,78]. One cause of this contradiction might be the relatively short time of the study in which the podocytes were treated with BK (3 hours and 6 hours), where we could not observe signs of cell death this early on in treatment. While the "Microtubule Dynamics" was suggested to be upregulated and the "Transport of Molecules" suggested to be downregulated, cytoskeletal activity plays a role in podocyte function and death, where podocyte detachment goes hand-in-hand with podocyte loss and progression of kidney disease [101].

Our study has shown that COX-2 is upregulated by BK treatment through several ways. First of all, the immunoblot with the COX-2 antibody showed a significant upregulation of COX-2 expression levels at 6 hours, as it has been suggested in previous studies before, but not in podocytes. Second, the PGE_2 metabolite, which is the product of COX-2 activity, was measured in the cell media by EIA, and shown to be increased, peaking at 24 hours, while treatment of podocytes with the COX general inhibitor Ibuprofen has shown a greatly decreased level of PGE_2 metabolite in the media at short-time (5 minutes) and longer treatment times (6 hours). These 2 results confirm the proteomic analysis showing an upregulation of COX-2 protein levels at short time (3 to 6 hours) due to BK treatment. Furthermore, other studies have demonstrated that p42/44 MAPK (ERK) lies downstream of the BDKRB receptor [102], and our results have supported that ERK gets phosphorylated at short-time (5 minutes – 30 minutes). Moreover, the PGE_2 levels measured in the media are significantly less in podocytes treated with a combination of BK and the ERK inhibitor PD98059 compared to podocytes treated with

BK alone, both at short time treatment (5 minutes) and at longer times (6 hours). These results confirm the position of ERK in the signaling pathway downstream of the BK receptor, but upstream of COX-2. Systems biology has shown us proteins of interest that are linked to COX-2. We investigated some of these proteins of interest that hold an important position in the propagation of diabetic nephropathy. One such protein is Nephrin, present at the slit diaphragm, and crucial for podocyte viability and kidney function [41]. Nephrin is known to be downregulated in cases of glomerular injury [41,42], and it is supported by our immunoblot experiments that show a significant downregulation of Nephrin protein levels at 6 hours.

Future prospects for this study would include evaluating the expression of other proteins that have been tied to diabetic nephropathy in the literature and to COX-2 expression by the systems biology. One of such proteins is CTGF, where a study has suggested that CTGF inhibition attenuates proteinuria [37], while another study has shown an increase in CTGF mRNA and protein level in a puromycin aminonucleoside nephrosis (PAN) and focal segmental glomerulosclerosis model [35]. Another future perspective would be the evaluation of the exact position of the Nephrin and CTGF proteins in the BK/COX-2 signaling pathway, whether they are upstream, downstream, or unrelated to COX-2 signaling. We could also evaluate the temporal changes in Nephrin protein expression that accompany BK treatment. This could be done with simple inhibition experiments with the Ibuprofen and PD98059 inhibitors followed by immunoblotting, or from a different angle, can be done by inhibiting the PGE_2 receptors EP_1-EP_4, then stimulating with BK and observing Nephrin expression. Furthermore, should the Ibuprofen lead to a higher Nephrin level than with BK treatment alone, we could potentially evaluate

the role of Ibuprofen as a renoprotective molecule since Nephrin downregulation has been established as a sign of renal damage [41,42]. Another prospective study would be the establishment of a COX-2 transgenic mouse, and the comparison between the COX-2 overexpressed podocyte cell line and the BK-treated cell line, as well as monitoring any difference in the progression of diabetic nephropathy between a normal mouse, a diabetic mouse, and a transgenic mouse for COX-2. The point of these experiments would be to evaluate if the COX-2 upregulation is the key step in the development of the diabetic nephropathy phenotype.

REFERENCES:

1. WHO (2016) <Global report on diabetes.pdf>.
2. ADA (2013) Economic Costs of Diabetes in the U.S. in 2012. Diabetes Care 36: 1033-1046.
3. Kleinberger JW, Pollin TI (2015) Personalized medicine in diabetes mellitus: current opportunities and future prospects. Annals of the New York Academy of Sciences 1346: 45-56.
4. Karalliedde J, Gnudi L (2016) Diabetes mellitus, a complex and heterogeneous disease, and the role of insulin resistance as a determinant of diabetic kidney disease. Nephrology Dialysis Transplantation 31: 206-213.
5. Jensen LA, Chik CL, Ryan EA (2016) Review of gestational diabetes mellitus effects on vascular structure and function. Diabetes and Vascular Disease Research 13: 170-182.
6. Lv X, Lv G-H, Dai G-Y, Sun H-M, Xu H-Q (2016) Food-advanced glycation end products aggravate the diabetic vascular complications via modulating the AGEs/RAGE pathway. Chinese Journal of Natural Medicines 14: 844-855.
7. Singh VP, Bali A, Singh N, Jaggi AS (2014) Advanced Glycation End Products and Diabetic Complications. The Korean Journal of Physiology & Pharmacology : Official Journal of the Korean Physiological Society and the Korean Society of Pharmacology 18: 1-14.
8. Domingueti CP, Dusse LMSA, Carvalho MdG, de Sousa LP, Gomes KB, et al. (2016) Diabetes mellitus: The linkage between oxidative stress, inflammation, hypercoagulability and vascular complications. Journal of Diabetes and its Complications 30: 738-745.
9. Giannini C, Mohn A, Chiarelli F, Kelnar CJH (2011) Macrovascular angiopathy in children and adolescents with type 1 diabetes. Diabetes/Metabolism Research and Reviews 27: 436-460.
10. The Emerging Risk Factors C (2010) Diabetes mellitus, fasting blood glucose concentration, and risk of vascular disease: a collaborative meta-analysis of 102 prospective studies. Lancet 375: 2215-2222.
11. Spencer EA, Pirie KL, Stevens RJ, Beral V, Brown A, et al. (2008) Diabetes and modifiable risk factors for cardiovascular disease: the prospective Million Women Study. European Journal of Epidemiology 23: 793.
12. Huxley R, Barzi F, Woodward M (2006) Excess risk of fatal coronary heart disease associated with diabetes in men and women: meta-analysis of 37 prospective cohort studies. BMJ : British Medical Journal 332: 73-78.
13. Kanaya AM, Grady D, Barrett-Connor E (2002) Explaining the sex difference in coronary heart disease mortality among patients with type 2 diabetes mellitus: A meta-analysis. Archives of Internal Medicine 162: 1737-1745.
14. Pedicino D, Liuzzo G, Trotta F, Giglio AF, Giubilato S, et al. (2013) Adaptive Immunity, Inflammation, and Cardiovascular Complications in Type 1 and Type 2 Diabetes Mellitus. Journal of Diabetes Research 2013: 184258.
15. Goldberg RB (2009) Cytokine and Cytokine-Like Inflammation Markers, Endothelial Dysfunction, and Imbalanced Coagulation in Development of Diabetes and Its Complications. The Journal of Clinical Endocrinology & Metabolism 94: 3171-3182.
16. Stitt AW, Curtis TM, Chen M, Medina RJ, McKay GJ, et al. (2016) The progress in understanding and treatment of diabetic retinopathy. Progress in Retinal and Eye Research 51: 156-186.

17. Yau JWY, Rogers SL, Kawasaki R, Lamoureux EL, Kowalski JW, et al. (2012) Global Prevalence and Major Risk Factors of Diabetic Retinopathy. Diabetes Care 35: 556-564.
18. Zheng Y, He M, Congdon N (2012) The worldwide epidemic of diabetic retinopathy. Indian Journal of Ophthalmology 60: 428-431.
19. Kobrin Klein BE (2007) Overview of Epidemiologic Studies of Diabetic Retinopathy. Ophthalmic Epidemiology 14: 179-183.
20. Javed S, Alam U, Malik RA (2015) Burning through the pain: treatments for diabetic neuropathy. Diabetes, Obesity and Metabolism 17: 1115-1125.
21. Fukami K, Yamagishi S-i, Ueda S, Okuda S (2008) Role of AGEs in Diabetic Nephropathy. Current Pharmaceutical Design 14: 946-952.
22. Russell JW, Zilliox LA (2014) Diabetic Neuropathies. Continuum : Lifelong Learning in Neurology 20: 1226-1240.
23. Bjornstad P, Cherney D, Maahs DM (2014) Early Diabetic Nephropathy in Type 1 Diabetes – New Insights. Current opinion in endocrinology, diabetes, and obesity 21: 279-286.
24. Borch-Johnsen K, Kreiner S (1987) Proteinuria: value as predictor of cardiovascular mortality in insulin dependent diabetes mellitus. British Medical Journal (Clinical research ed) 294: 1651-1654.
25. Sasso FC, Chiodini P, Carbonara O, De Nicola L, Conte G, et al. (2012) High cardiovascular risk in patients with Type 2 diabetic nephropathy: the predictive role of albuminuria and glomerular filtration rate. The NID-2 Prospective Cohort Study. Nephrology Dialysis Transplantation 27: 2269-2274.
26. Tanaka N, Babazono T, Takagi M, Yoshida N, Toya K, et al. (2015) Albuminuria and reduced glomerular filtration rate for predicting the renal outcomes in type 2 diabetic patients. Nephrology 20: 531-538.
27. Guo K, Lu J, Kou J, Wu M, Zhang L, et al. (2015) Increased urinary Smad3 is significantly correlated with glomerular hyperfiltration and a reduced glomerular filtration rate and is a new urinary biomarker for diabetic nephropathy. BMC Nephrology 16: 159.
28. Žeravica R, Čabarkapa V, Ilinčić B, Sakač V, Mijović R, et al. (2015) Plasma endothelin-1 level, measured glomerular filtration rate and effective renal plasma flow in diabetic nephropathy. Renal Failure 37: 681-686.
29. Suzuki D, Toyoda M, Yamamoto N, Miyauchi M, Katoh M, et al. (2006) Relationship between the Expression of Advanced Glycation End-Products (AGE) and the Receptor for AGE (RAGE) mRNA in Diabetic Nephropathy. Internal Medicine 45: 435-441.
30. Pagtalunan ME, Miller PL, Jumping-Eagle S, Nelson RG, Myers BD, et al. (1997) Podocyte loss and progressive glomerular injury in type II diabetes. Journal of Clinical Investigation 99: 342-348.
31. Guan TH, Chen G, Gao B, Janssen MR, Uttarwar L, et al. (2013) Caveolin-1 deficiency protects against mesangial matrix expansion in a mouse model of type 1 diabetic nephropathy. Diabetologia 56: 2068-2077.
32. Weil EJ, Lemley KV, Mason CC, Yee B, Jones LI, et al. (2012) Podocyte detachment and reduced glomerular capillary endothelial fenestration promote kidney disease in type 2 diabetic nephropathy. Kidney international 82: 1010-1017.
33. de las Heras N, Ruiz-Ortega M, Rupérez M, Sanz-Rosa D, Miana M, et al. (2006) Role of connective tissue growth factor in vascular and renal damage associated with hypertension in rats. Interactions with angiotensin II. Journal of the Renin-Angiotensin-Aldosterone System 7: 192-200.

34. Lu W, Liu S, Zhao Z, Liu Y, Li T (2014) The effect of connective tissue growth factor on renal fibrosis and podocyte injury in hypertensive rats. Renal Failure 36: 1420-1427.
35. Fuchshofer R, Ullmann S, Zeilbeck LF, Baumann M, Junglas B, et al. (2011) Connective tissue growth factor modulates podocyte actin cytoskeleton and extracellular matrix synthesis and is induced in podocytes upon injury. Histochemistry and Cell Biology 136: 301.
36. Umezono T, Toyoda M, Kato M, Miyauchi M, Kimura M, et al. (2006) Glomerular expression of CTGF, TGF-beta 1 and type IV collagen in diabetic nephropathy. JOURNAL OF NEPHROLOGY 19: 751-757.
37. Dai HY, Zheng M, Lv LL, Tang RN, Ma KL, et al. (2012) The roles of connective tissue growth factor and integrin-linked kinase in high glucose-induced phenotypic alterations of podocytes. J Cell Biochem 113: 293-301.
38. Turk T, Leeuwis JW, Gray J, Torti SV, Lyons KM, et al. (2009) BMP Signaling and Podocyte Markers Are Decreased in Human Diabetic Nephropathy in Association With CTGF Overexpression. Journal of Histochemistry and Cytochemistry 57: 623-631.
39. Baelde HJ, Eikmans M, Lappin DWP, Doran PP, Hohenadel D, et al. (2007) Reduction of VEGF-A and CTGF expression in diabetic nephropathy is associated with podocyte loss. Kidney international 71: 637-645.
40. Wang P, Li M, Liu Q, Chen B, Ji Z (2015) Detection of urinary podocytes and nephrin as markers for children with glomerular diseases. Experimental Biology and Medicine 240: 169-174.
41. Li X, Chuang PY, D'Agati VD, Dai Y, Yacoub R, et al. (2015) Nephrin Preserves Podocyte Viability and Glomerular Structure and Function in Adult Kidneys. Journal of the American Society of Nephrology : JASN 26: 2361-2377.
42. Yu S (2016) Role of nephrin in podocyte injury induced by angiotension II. Journal of Receptors and Signal Transduction 36: 1-5.
43. Agrawal S, Guess AJ, Chanley MA, Smoyer, William E (2014) Albumin-induced podocyte injury and protection are associated with regulation of COX-2. Kidney international 86: 1150-1160.
44. Pathak M, Wong SS, Dreveny I, Emsley J (2013) Structure of plasma and tissue kallikreins. Thrombosis and haemostasis 110: 423-433.
45. Björkqvist J, Jämsä A, Renné T (2013) Plasma kallikrein: the bradykinin-producing enzyme. Thrombosis and haemostasis 110: 399-407.
46. Feener EP, Zhou Q, Fickweiler W (2013) Role of plasma kallikrein in diabetes and metabolism. Thrombosis and haemostasis 110: 434-441.
47. Zhao Y, Qiu Q, Mahdi F, Shariat-Madar Z, Røjkjær R, et al. (2001) Assembly and activation of HK-PK complex on endothelial cells results in bradykinin liberation and NO formation. American Journal of Physiology - Heart and Circulatory Physiology 280: H1821-H1829.
48. Kolte D, Shariat-Madar Z (2016) Plasma Kallikrein Inhibitors in Cardiovascular Disease: An Innovative Therapeutic Approach. Cardiology in Review 24: 99-109.
49. Shariat-Madar Z, Mahdi F, Schmaier AH (2002) Identification and Characterization of Prolylcarboxypeptidase as an Endothelial Cell Prekallikrein Activator. Journal of Biological Chemistry 277: 17962-17969.
50. Gailani D, Renné T (2007) Intrinsic Pathway of Coagulation and Arterial Thrombosis. Arteriosclerosis, Thrombosis, and Vascular Biology 27: 2507-2513.
51. Colman RW (1969) Activation of plasminogen by human plasma kallikrein. Biochemical and Biophysical Research Communications 35: 273-279.

52. DiScipio RG (1982) The activation of the alternative pathway C3 convertase by human plasma kallikrein. Immunology 45: 587-595.
53. Selvarajan S, Lund LR, Takeuchi T, Craik CS, Werb Z (2001) A plasma kallikrein-dependent plasminogen cascade required for adipocyte differentiation. Nature cell biology 3: 267-275.
54. Lieb W, Chen M-H, Teumer A, de Boer RA, Lin H, et al. (2015) Genome-Wide Meta-Analyses of Plasma Renin Activity and Concentration Reveal Association with the Kininogen 1 and Prekallikrein Genes. Circulation Cardiovascular genetics 8: 131-140.
55. Regoli D, Gobeil Jr F (2015) Critical insights into the beneficial and protective actions of the kallikrein–kinin system. Vascular Pharmacology 64: 1-10.
56. Koumandou VL, Scorilas A (2013) Evolution of the Plasma and Tissue Kallikreins, and Their Alternative Splicing Isoforms. PLoS ONE 8: e68074.
57. Maurer M, Bader M, Bas M, Bossi F, Cicardi M, et al. (2011) New topics in bradykinin research. Allergy 66: 1397-1406.
58. Pereira RL, Felizardo RJF, Cenedeze MA, Hiyane MI, Bassi ÊJ, et al. (2014) Balance between the two kinin receptors in the progression of experimental focal and segmental glomerulosclerosis in mice. Disease Models & Mechanisms 7: 701-710.
59. Asmis LM, Sulzer I, Furlan M, Lämmle B (2002) Prekallikrein deficiency: The characteristic normalization of the severely prolonged aPTT following increased preincubation time is due to autoactivation of factor XII. Thrombosis Research 105: 463-470.
60. Patrassi GM, Vettor R, Padovan D, Girolami A (1982) Contact phase of blood coagulation in diabetes mellitus. European Journal of Clinical Investigation 12: 307-311.
61. Abdulaal M, Haddad NMN, Sun JK, Silva PS (2016) The Role of Plasma Kallikrein–Kinin Pathway in the Development of Diabetic Retinopathy: Pathophysiology and Therapeutic Approaches. Seminars in Ophthalmology 31: 19-24.
62. Jaffa MA, Kobeissy F, Al Hariri M, Chalhoub H, Eid A, et al. (2012) Global Renal Gene Expression Profiling Analysis in B(2)-Kinin Receptor Null Mice: Impact of Diabetes. PLoS ONE 7: e44714.
63. Tan Y, Keum J-S, Wang B, McHenry MB, Lipsitz SR, et al. (2007) Targeted deletion of B2-kinin receptors protects against the development of diabetic nephropathy. American Journal of Physiology - Renal Physiology 293: F1026.
64. Kakoki M, Takahashi N, Jennette JC, Smithies O (2004) Diabetic nephropathy is markedly enhanced in mice lacking the bradykinin B2 receptor. Proceedings of the National Academy of Sciences of the United States of America 101: 13302-13305.
65. Kakoki M, Sullivan KA, Backus C, Hayes JM, Oh SS, et al. (2010) Lack of both bradykinin B1 and B2 receptors enhances nephropathy, neuropathy, and bone mineral loss in Akita diabetic mice. Proceedings of the National Academy of Sciences of the United States of America 107: 10190-10195.
66. Silva AR, Larangeira AP, Pacheco P, Calixto JB, Henriques MGMO, et al. (1999) Bradykinin down-regulates LPS-induced eosinophil accumulation in the pleural cavity of mice through type 2-kinin receptor activation: a role for prostaglandins. British Journal of Pharmacology 127: 569-575.
67. Frungieri MB, Calandra RS, Mayerhofer A, Matzkin ME (2015) Cyclooxygenase and prostaglandins in somatic cell populations of the testis. Reproduction 149: R169-R180.

68. Greenhough A, Smartt HJM, Moore AE, Roberts HR, Williams AC, et al. (2009) The COX-2/PGE 2 pathway: key roles in the hallmarks of cancer and adaptation to the tumour microenvironment. Carcinogenesis 30: 377-386.
69. Claar D, Hartert TV, Peebles RS (2015) The Role of Prostaglandins in Allergic Lung Inflammation and Asthma. Expert review of respiratory medicine 9: 55-72.
70. Dixon DA, Blanco FF, Bruno A, Patrignani P (2013) Chapter 2: Mechanistic Aspects of COX-2 Expression in Colorectal Neoplasia. Recent results in cancer research Fortschritte der Krebsforschung Progres dans les recherches sur le cancer 191: 7-37.
71. Alhouayek M, Muccioli GG (2014) COX-2-derived endocannabinoid metabolites as novel inflammatory mediators. Trends in Pharmacological Sciences 35: 284-292.
72. Figueiredo-Pereira ME, Corwin C, Babich J (2016) Prostaglandin J2: a potential target for halting inflammation-induced neurodegeneration. Annals of the New York Academy of Sciences 1363: 125-137.
73. Cheng H, Fan X, Moeckel GW, Harris RC (2011) Podocyte COX-2 Exacerbates Diabetic Nephropathy by Increasing Podocyte (Pro)renin Receptor Expression. Journal of the American Society of Nephrology : JASN 22: 1240-1251.
74. Simmons DL, Botting RM, Hla T (2004) Cyclooxygenase Isozymes: The Biology of Prostaglandin Synthesis and Inhibition. Pharmacological Reviews 56: 387-437.
75. Trappe TA, Liu SZ (2013) Effects of prostaglandins and COX-inhibiting drugs on skeletal muscle adaptations to exercise. Journal of Applied Physiology 115: 909-919.
76. Duffy DM (2015) Novel contraceptive targets to inhibit ovulation: the prostaglandin E2 pathway. Human Reproduction Update 21: 652-670.
77. Tachikawa M, Hosoya K-i, Terasaki T (2014) Chapter Eleven - Pharmacological Significance of Prostaglandin E2 and D2 Transport at the Brain Barriers. In: Thomas PD, editor. Advances in Pharmacology: Academic Press. pp. 337-360.
78. Jia Z, Zhang Y, Ding G, Heiney KM, Huang S, et al. (2015) Role of COX-2/mPGES-1/Prostaglandin E2 Cascade in Kidney Injury. Mediators of Inflammation 2015: 147894.
79. Srivastava T, Alon US, Cudmore PA, Tarakji B, Kats A, et al. (2014) Cyclooxygenase-2, prostaglandin E2, and prostanoid receptor EP2 in fluid flow shear stress-mediated injury in the solitary kidney. American Journal of Physiology - Renal Physiology 307: F1323.
80. Faour WH, Gomi K, Kennedy CRJ (2008) PGE2 induces COX-2 expression in podocytes via the EP4 receptor through a PKA-independent mechanism. Cellular Signalling 20: 2156-2164.
81. Maubach KA, Grundy D (1999) The role of prostaglandins in the bradykinin-induced activation of serosal afferents of the rat jejunum in vitro. The Journal of Physiology 515: 277-285.
82. Förstermann U, Hertting G, Neufang B (1986) The role of endothelial and non-endothelial prostaglandins in the relaxation of isolated blood vessels of the rabbit induced by acetylcholine and bradykinin. British Journal of Pharmacology 87: 521-532.
83. López-Villar E, Martos-Moreno GÁ, Chowen JA, Okada S, Kopchick JJ, et al. (2015) A proteomic approach to obesity and type 2 diabetes. Journal of Cellular and Molecular Medicine 19: 1455-1470.
84. White KE, Bilous RW, Marshall SM, El Nahas M, Remuzzi G, et al. (2002) Podocyte Number in Normotensive Type 1 Diabetic Patients With Albuminuria. Diabetes 51: 3083-3089.
85. Jaffa AA, Miller BS, Rosenzweig SA, Naidu PS, Velarde V, et al. (1997) Bradykinin induces tubulin phosphorylation and nuclear translocation of MAP kinase in mesangial cells. American Journal of Physiology - Renal Physiology 273: F916-F924.

86. Tang SCW, Chan LYY, Leung JCK, Cheng AS, Lan HY, et al. (2011) Additive renoprotective effects of B2-kinin receptor blocker and PPAR-[gamma] agonist in uninephrectomized db/db mice. Lab Invest 91: 1351-1362.
87. Tan Y, Keum J-S, Wang B, McHenry MB, Lipsitz SR, et al. (2007) Targeted deletion of B₂-kinin receptors protects against the development of diabetic nephropathy. American Journal of Physiology - Renal Physiology 293: F1026-F1035.
88. Habib A, Créminon C, Frobert Y, Grassi J, Pradelles P, et al. (1993) Demonstration of an inducible cyclooxygenase in human endothelial cells using antibodies raised against the carboxyl-terminal region of the cyclooxygenase-2. Journal of Biological Chemistry 268: 23448-23454.
89. Kreisberg JI, Hoover RL, Karnovsky MJ (1978) Isolation and characterization of rat glomerular epithelial cells in vitro. Kidney international 14: 21-30.
90. Bolla M, You D, Loufrani L, Levy BI, Levy-Toledano S, et al. (2004) Cyclooxygenase involvement in thromboxane-dependent contraction in rat mesenteric resistance arteries. Hypertension 43: 1264-1269.
91. Jatho A, Hartmann S, Kittana N, Mügge F, Wuertz CM, et al. (2015) RhoA Ambivalently Controls Prominent Myofibroblast Characteritics by Involving Distinct Signaling Routes. PLoS ONE 10: e0137519.
92. Brosius FC, Coward RJ (2014) Podocytes, Signaling Pathways, and Vascular Factors in Diabetic Kidney Disease. Advances in chronic kidney disease 21: 304-310.
93. Huang Z, Zhang L, Chen Y, Zhang H, Yu C, et al. (2016) RhoA deficiency disrupts podocyte cytoskeleton and induces podocyte apoptosis by inhibiting YAP/dendrin signal. BMC Nephrology 17: 66.
94. Park SJ, Ahn E-M, Ha T-S, Shin JI (2014) Beta-Catenin and Its Alteration in an Experimental Model of Diabetic Nephropathy.
95. Kanasaki K, Kanda Y, Palmsten K, Tanjore H, Lee SB, et al. (2008) Integrin β1 Mediated Matrix Assembly and Signaling is Critical for the Normal Development and Function of the Kidney Glomerulus. Developmental biology 313: 584-593.
96. Kettwig M, Schubach M, Zimmermann FA, Klinge L, Mayr JA, et al. (2015) From ventriculomegaly to severe muscular atrophy: Expansion of the clinical spectrum related to mutations in AIFM1. Mitochondrion 21: 12-18.
97. Lu D-Y, Leung Y-M, Huang S-M, Wong K-L (2010) Bradykinin-induced cell migration and COX-2 production mediated by the bradykinin B1 receptor in glioma cells. J Cell Biochem 110: 141-150.
98. Deacon K, Knox AJ (2015) Human airway smooth muscle cells secrete amphiregulin via bradykinin/COX-2/PGE(2), inducing COX-2, CXCL8, and VEGF expression in airway epithelial cells. American Journal of Physiology - Lung Cellular and Molecular Physiology 309: L237-L249.
99. Rodriguez JA, Vio CP, Pedraza PL, McGiff JC, Ferreri NR (2004) Bradykinin Regulates Cyclooxygenase-2 in Rat Renal Thick Ascending Limb Cells. Hypertension 44: 230.
100. More AS, Kim HM, Zhao R, Khang G, Hildebrandt T, et al. (2014) COX-2 mediated induction of endothelium-independent contraction to bradykinin in endotoxin-treated porcine coronary artery. J Cardiovasc Pharmacol 64: 209-217.
101. Kriz W, Lemley KV (2015) A Potential Role for Mechanical Forces in the Detachment of Podocytes and the Progression of CKD. Journal of the American Society of Nephrology : JASN 26: 258-269.

102. Webb JG, Tan Y, Jaffa MA, Jaffa AA (2010) Evidence for Prostacyclin and cAMP Upregulation by Bradykinin and Insulin-Like Growth Factor 1 in Vascular Smooth Muscle Cells. Journal of receptor and signal transduction research 30: 61-71.